STRUCTURAL LOADS IN A MODEL GRAIN BIN DURING DRYING OF STORED GRAIN WITH NEAR-AMBIENT AIR

BY

YUQIN SHAN

A thesis
Submitted to the Faculty of Graduate Studies
in partial fulfilment of the requirements
for the degree of

MASTER OF SCIENCE

Department of Biosystems Engineering
University of Manitoba
Winnipeg, Manitoba

ISBN 0-612-16286-9

Name _____

Dissertation Abstracts International and *Masters Abstracts International* are arranged by broad, general subject categories. Please select the one subject which most nearly describes the content of your dissertation or thesis. Enter the corresponding four-digit code in the spaces provided.

SUBJECT TERM

Agricultural Egineering

SUBJECT CODE 0539 UMI

Subject Categories

THE HUMANITIES AND SOCIAL SCIENCES

COMMUNICATIONS AND THE ARTS
Architecture 0729
Art History 0377
Cinema 0900
Dance 0378
Design and Decorative Arts 0389
Fine Arts 0357
Information Science 0723
Journalism 0391
Landscape Architecture 0390
Library Science 0399
Mass Communications 0708
Music 0413
Speech Communication 0459
Theater 0465

EDUCATION
General 0515
Administration 0514
Adult and Continuing 0516
Agricultural 0517
Art 0273
Bilingual and Multicultural 0282
Business 0688
Community College 0275
Curriculum and Instruction 0727
Early Childhood 0518
Elementary 0524
Educational Psychology 0525
Finance 0277
Guidance and Counseling 0519
Health 0680
Higher 0745
History of 0520
Home Economics 0278
Industrial 0521
Language and Literature 0279
Mathematics 0280
Music 0522
Philosophy of 0998
Physical 0523
Reading 0535
Religious 0527
Sciences 0714
Secondary 0533
Social Sciences 0534
Sociology of 0340
Special 0529
Teacher Training 0530
Technology 0710
Tests and Measurements 0288
Vocational 0747

LANGUAGE, LITERATURE AND LINGUISTICS
Language
- General 0679
- Ancient 0289
- Linguistics 0290
- Modern 0291
- Rhetoric and Composition 0681

Literature
- General 0401
- Classical 0294
- Comparative 0295
- Medieval 0297
- Modern 0298
- African 0316
- American 0591
- Asian 0305
- Canadian (English) 0352
- Canadian (French) 0355
- Caribbean 0360
- English 0593
- Germanic 0311
- Latin American 0312
- Middle Eastern 0315
- Romance 0313
- Slavic and East European 0314

PHILOSOPHY, RELIGION AND THEOLOGY
Philosophy 0422
Religion
- General 0318
- Biblical Studies 0321
- Clergy 0319
- History of 0320
- Philosophy of 0322

Theology 0469

SOCIAL SCIENCES
American Studies 0323
Anthropology
- Archaeology 0324
- Cultural 0326
- Physical 0327

Business Administration
- General 0310
- Accounting 0272
- Banking 0770
- Management 0454
- Marketing 0338

Canadian Studies 0385
Economics
- General 0501
- Agricultural 0503
- Commerce-Business 0505
- Finance 0508
- History 0509
- Labor 0510
- Theory 0511

Folklore 0358
Geography 0366
Gerontology 0351
History
- General 0578
- Ancient 0579
- Medieval 0581
- Modern 0582
- Church 0330
- Black 0328
- African 0331
- Asia, Australia and Oceania 0332
- Canadian 0334
- European 0335
- Latin American 0336
- Middle Eastern 0333
- United States 0337

History of Science 0585
Law 0398
Political Science
- General 0615
- International Law and Relations 0616
- Public Administration 0617

Recreation 0814
Social Work 0452
Sociology
- General 0626
- Criminology and Penology 0627
- Demography 0938
- Ethnic and Racial Studies 0631
- Individual and Family Studies 0628
- Industrial and Labor Relations 0629
- Public and Social Welfare 0630
- Social Structure and Development 0700
- Theory and Methods 0344

Transportation 0709
Urban and Regional Planning 0999
Women's Studies 0453

THE SCIENCES AND ENGINEERING

BIOLOGICAL SCIENCES
Agriculture
- General 0473
- Agronomy 0285
- Animal Culture and Nutrition 0475
- Animal Pathology 0476
- Fisheries and Aquaculture 0792
- Food Science and Technology 0359
- Forestry and Wildlife 0478
- Plant Culture 0479
- Plant Pathology 0480
- Range Management 0777
- Soil Science 0481
- Wood Technology 0746

Biology
- General 0306
- Anatomy 0287
- Animal Physiology 0433
- Biostatistics 0308
- Botany 0309
- Cell 0379
- Ecology 0329
- Entomology 0353
- Genetics 0369
- Limnology 0793
- Microbiology 0410
- Molecular 0307
- Neuroscience 0317
- Oceanography 0416
- Plant Physiology 0817
- Veterinary Science 0778
- Zoology 0472

Biophysics
- General 0786
- Medical 0760

EARTH SCIENCES
Biogeochemistry 0425
Geochemistry 0996
Geodesy 0370
Geology 0372
Geophysics 0373
Hydrology 0388
Mineralogy 0411
Paleobotany 0345
Paleoecology 0426
Paleontology 0418
Paleozoology 0985
Palynology 0427
Physical Geography 0368
Physical Oceanography 0415

HEALTH AND ENVIRONMENTAL SCIENCES
Environmental Sciences 0768
Health Sciences
- General 0566
- Audiology 0300
- Dentistry 0567
- Education 0350
- Administration, Health Care 0769
- Human Development 0758
- Immunology 0982
- Medicine and Surgery 0564
- Mental Health 0347
- Nursing 0569
- Nutrition 0570
- Obstetrics and Gynecology 0380
- Occupational Health and Safety 0354
- Oncology 0992
- Ophthalmology 0381
- Pathology 0571
- Pharmacology 0419
- Pharmacy 0572
- Public Health 0573
- Radiology 0574
- Recreation 0575
- Rehabilitaion and Therapy 0382
- Speech Pathology 0460
- Toxicology 0383

Home Economics 0386

PHYSICAL SCIENCES
Pure Sciences
Chemistry
- General 0485
- Agricultural 0749
- Analytical 0486
- Biochemistry 0487
- Inorganic 0488
- Nuclear 0738
- Organic 0490
- Pharmaceutical 0491
- Physical 0494
- Polymer 0495
- Radiation 0754

Mathematics 0405
Physics
- General 0605
- Acoustics 0986
- Astronomy and Astrophysics 0606
- Atmospheric Science 0608
- Atomic 0748
- Condensed Matter 0611
- Electricity and Magnetism 0607
- Elementary Particles and High Energy 0798
- Fluid and Plasma 0759
- Molecular 0609
- Nuclear 0610
- Optics 0752
- Radiation 0756

Statistics 0463

Applied Sciences
Applied Mechanics 0346
Computer Science 0984
Engineering
- General 0537
- Aerospace 0538
- Agricultural 0539
- Automotive 0540
- Biomedical 0541
- Chemical 0542
- Civil 0543
- Electronics and Electrical 0544
- Environmental 0775
- Industrial 0546
- Marine and Ocean 0547
- Materials Science 0794
- Mechanical 0548
- Metallurgy 0743
- Mining 0551
- Nuclear 0552
- Packaging 0549
- Petroleum 0765
- Sanitary and Municipal 0554
- System Science 0790

Geotechnology 0428
Operations Research 0796
Plastics Technology 0795
Textile Technology 0994

PSYCHOLOGY
General 0621
Behavioral 0384
Clinical 0622
Cognitive 0633
Developmental 0620
Experimental 0623
Industrial 0624
Personality 0625
Physiological 0989
Psychobiology 0349
Psychometrics 0632
Social 0451

THE UNIVERSITY OF MANITOBA

FACULTY OF GRADUATE STUDIES

COPYRIGHT PERMISSION

STRUCTURAL LOADS IN A MODEL GRAIN BIN DURING DRYING OF STORED GRAIN WITH NEAR-AMBIENT AIR

BY

YUQIN SHAN

A Thesis/Practicum submitted to the Faculty of Graduate Studies of the University of Manitoba in partial fulfillment of the requirements for the degree of

MASTER OF SCIENCE

I hereby declare that I am the sole author of this thesis.

I authorized the University of Manitoba to lend this thesis to other institutions and/or individuals for the purpose of scholarly research.

Yuqin Shan

I further authorized the University of Manitoba to reproduce this thesis by photocopying or by other means, in total or in part, at the request of other institutions and/or individuals for the purpose of scholarly research.

Yuqin Shan

ABSTRACT

An experiment was conducted to study loads in grain bins during the drying of stored grain with near-ambient air. A corrugated steel model bin 0.96 m in diameter (an average of inner and outer peak circles of corrugates) and 1.57 m high was used in the experiment. Vertical forces on the bin floor and wall were measured separately with force transducers. Lateral and vertical pressures at three depths in the grain mass close to the bin wall were recorded using diaphragm pressure sensors. Freshly harvested hard red spring wheat was first dried by blowing near-ambient air through the grain bed and then three wetting-drying cycles were performed. Wetting processes were conducted by blowing near-saturated air through the grain bulk.

Measured static pressures at three depths were in agreement with Janssen's predictions and average lateral to vertical pressure ratio (K) was 0.47. During the initial drying process from a moisture content of 14.1% to an average of 11.0% db, changes in vertical forces on the floor and wall were negligible. Wetting of stored grain in an average moisture range of 8.7% to 19.7% caused significant changes in bin loads. The greatest peak/static ratio of vertical force on the floor was 2.7. The upward force of grain swelling reversed the direction of vertical frictional force on the wall from downward to upward. The greatest upward force on the wall reached 5.98 kN, which was 1.6 times as great as the static wall load. The greatest increase in lateral pressure occurred at the bottom level from 3.54 to 31.95 kPa. The greatest overpressure factor was 10.6. Vertical pressure at the top level had the greatest change, from 3.03 to 20.23 kPa or 6.7 fold. The highest lateral to vertical pressure ratio was 1.95, which occurred at the bottom level.

ACKNOWLEDGEMENTS

Throughout my thesis project, I received assistance, suggestions, and encouragement from many individuals. Their inspiration and help were sincerely appreciated.

First, I thank Dr. Q. Zhang, my advisor, for his invaluable guidance, suggestions and encouragement during the whole process of this project. His positive attitude always encouraged me to go further and was very much appreciated. Thank you also to Dr. M.G. Britton and Dr. N. Rajapakse for their time evaluating my thesis and for their invaluable suggestions.

A special thank you to Mr. J. Putnam, Mr. M. McDonald, Mr. R. Ataman, Mr. J. Philp, and my fellow students for their help and suggestions during the periods of building the test system and running the experiment. A sincere thank you to Dr. W.E. Muir for loaning me the papers and unpublished data. Assistance from Ms. D. Bialek and Ms. D. Watson was also acknowledged.

The financial support from the National Science and Engineering Research Council of Canada was gratefully acknowledged.

Finally, I thank my wife, L. Wang, for her patience and support.

TABLE OF CONTENTS

LIST OF TABLES

LIST OF FIGURES

Chapter 1

INTRODUCTION

When a grain bin is filled with grain, loads (vertical and lateral pressures and frictional force) are exerted on the bin structure by the grain. These bin loads are classified as being static or dynamic. As implied by the name, static loads occur when interaction between grain and storage structure is at rest. Dynamic loads are induced when the static state is broken, which can be caused by filling and emptying of grain, wind, rain, snow, vibration, rapid declines of ambient temperature, and changes in properties of stored grain. In bin load studies, the ratio of peak dynamic to static pressure is termed as overpressure factor (OPF). The ratio of peak dynamic to static vertical frictional force on the wall (DSR) is also commonly introduced to describe dynamic loads. To design structurally sound and economic grain bins, both static and dynamic loads should be accurately predicted. Moisture induced loads are among the most important dynamic loads which need to be studied.

Rainfall during harvest in the grain growing areas often forces farmers to store grain with above-safety moisture contents. Near-ambient air drying is a common practice to protect the grain from spoilage due to microfloral infection and biochemical degradation and to prolong the period of its safe storage (Otten et al. 1977; Muir et al. 1991; Zhang and Britton 1994). During drying, near-ambient air is blown through the grain bulk to lower the temperature and moisture of grain. To achieve a safe storage moisture of grain, drying usually continues for several months. During this period of time, variable weather conditions may cause the relative humidity (RH) of air to fluctuate

in a wide range. When the RH of the air is lower than the equilibrium relative humidity (ERH) of the grain, moisture is removed from the grain; Conversely, when the RH of the air is higher, moisture is added to the grain. Thus, the grain may be subjected to both drying and wetting. When grain is dried, grain kernels shrink and grain bulk contracts. When grain is wetted, grain kernels swell and grain bed expands. Both the contraction and expansion of grain bulk may cause variations in bin loads. Especially during wetting, the swelling of grain is restricted by the bin wall, thus high pressures may be induced on the wall. This extra bin wall load may cause structure failures of the grain bin. Furthermore, moisture content affects grain internal friction and grain to wall friction, which in turn affects bin loads.

Miller (1984) cautioned that grain swelling through changes in moisture content could cause cracking of concrete silos or buckling of steel bins. Trahair (1985) pointed out that there are some unrecognised loading conditions which may lead to failures. Examples are internal pressurization resulting from fumigation or ventilation equipment, and swelling of agricultural products resulting from moisture ingress. Britton et al. (1993) reported that field observations of corrugated steel bins had revealed a relatively high occurrence of "recorrugation" in the walls just above drying floors. But, little information on moisture induced bin loads can be found in design standards and codes to assist the designers.

In this study, loads induced on bin structures due to grain moisture changes, termed moisture induced loads, were investigated for the drying and wetting of stored wheat.

Chapter 2

LITERATURE REVIEW

2.1 Theories of Static Loads

Grain bins are historically classified as shallow bins and deep bins. A deep bin is defined as having a height to diameter ratio greater than 0.75 (Ketchum 1919; Isaacson and Boyd 1965; NRCC 1977 & 1983). Bins of which the ratio is less than 0.75 are considered as shallow bins. Grain pressure research at the early stage focused primarily on static loads.

2.1.1 Pressure Theories for Shallow Bins

Prior to 1850, Rankine's formula was commonly used for shallow bin design. Rankine established his equation based on the hydrostatic pressure theory (Ketchum 1919). It was assumed that lateral pressure on the retaining wall increased linearly with the grain depth and there was no friction between grain and wall. This theory can be applied only under the conditions of level filled grain and vertical wall. Coulomb extended the theory to the case of heaped fill of grain and inclined bin wall (Ketchum 1919).

2.1.2 Pressure Theories for Deep Bins

Janssen performed the first theoretical analysis of grain pressures in 1895 (Ketchum, 1919). Based on the assumptions of a constant friction coefficient of grain on the wall, a constant bulk density, and a constant ratio of lateral to vertical pressures, the Janssen equation was yielded as follows:

$$V = \frac{wgR}{\mu K}\left(1 - \exp^{-\frac{\mu KY}{R}}\right) \qquad (1)$$

$$L=KV \tag{2}$$

where V = vertical pressure of grain at depth Y (kPa),

L = lateral pressure of grain at depth Y (kPa),

w = bulk density of grain (kg/m^3),

g = gravity acceleration constant, $9.8*10^{-3}$ (kN/kg),

R = hydraulic radius of bin (m),

μ = friction coefficient of grain to wall,

K = ratio of lateral to vertical pressure, and

Y = depth measured from the free surface of grain (m).

Airy (1897, cited by Ketchum 1919) proposed a formula for calculation of grain pressure based on the theory of sliding wedges, which gave results similar to Janssen's but never gained wide acceptance due to its complexity.

In the 1940's, another set of equations for grain pressure predictions were developed by the Reimbert brothers. The detailed derivation was found in Reimbert and Reimbert (1976). By considering the ratio of lateral to vertical pressure as the function of the grain depth, they defined a hyperbolic equation which has the same set of variables as Janssen's equation:

$$V=wgY\left(\frac{Y\mu K}{R}+1\right)^{-1} \tag{3}$$

$$L=\frac{wgR}{\mu}\left[1-\left(\frac{Y\mu K}{R}+1\right)^{-2}\right] \tag{4}$$

Later on, based on the fact that the grain property parameters, w, μ, and K, are variables instead of constants, many other researchers derived new theories or modified existing equations to predict static pressures (Walker 1966; Hancock and Nedderman 1974; Cowin 1977; and Ross et al. 1979). However, Janssen's formulas still remain to be the simplest and the most direct method for predicting static grain pressures and are extensively used in design standards and codes to determine static loads. The Reimberts' equations are selected as an alternative in some codes.

2.2 Experimental Determination of Bin Loads

Experimental determination of bin loads has been an attractive subject to many researchers. Some investigators measured vertical forces on the floor and wall by supporting the floor and wall separately and then computed the lateral force on the wall by assuming the coefficient friction of grain on the bin wall (Janssen 1895; Jamieson 1903; Reimbert and Reimbert 1976). This only provides average values of vertical bin loads which are not meaningful in designing grain bins.

Collin and Peschl (1963) mounted two-element rosette strain gages on the wall of a model bin made of "building aluminium" sheets to measure static and dynamic loads. They concluded that the method of determining pressures indirectly by using strain gages was possible, but large strain readings were desired for precision. Smith and Simmonds (1983) fixed strain gages on steel reinforcement in concrete bins to determine pressure on the bin wall. Williams et al. (1987) mounted diaphragm transducers flush to the bin wall to give direct stress values. However, their measured values were unstable because wall flexibility distorted the test results and strain magnitudes were small (Atewologun

and Riskowski 1991).

Some other researchers have shown successful pressure measurements within the mass of a granular material (Galili and Tompson 1989; William et al. 1989; Tompson and Williams 1990; Atewologun and Riskowski 1991). In-mass stress measurements have the advantage of measuring existing pressure directly thus excluding the influence of the unknown factors.

2.3 Studies on Grain Properties and Grain-structure Interactions

Knowledge on stress-strain behaviour of grain and grain-structure interactions plays a key role in predicting grain bin loads. Stress-strain behaviour of grain is dependent on its physical states, such as moisture content and bulk density. Grain-structure interactions are affected by the properties of both the stored material and structure materials. The most frequently studied material property parameters and grain-structure interactions include bulk density, friction coefficient, and ratio of lateral to vertical pressure which may be derived from the internal friction of material. For a given storage structure, these parameters define structural loads.

2.3.1 Bulk Density

Bulk density is the mass of grain divided by the volume occupied by the grain and intergranular space. Bulk density is a function of moisture content. Miles (1937) investigated the test weight (bulk density) of corn at moisture contents between 10 and 40%. He found that the minimum test weight occurred at 30-31% moisture content and that there was a higher test weight for greater moisture contents. Differences in test weight at same moisture were greater when corn was first dried and rewetted than that

during subsequent drying and rewetting. Bushuk and Hlynka (1960) observed considerable hysteresis in weight and volume changes in wheat during adsorption and desorption of moisture. Browne (1962) measured rewetted wheat, barley, and oats at 10 to 30% moisture content (wb). He found that bulk density decreased with increases in moisture content. Chung and Converse (1971) measured the test weight of corn between 9 and 27% and wheat between 9 and 19% moisture content. Differences in test weight during absorption and desorption were small for wheat. The hysteresis differences were greater for corn than those for wheat. Gustafason and Hall (1972) presented numerous data on the true (kernel) density and porosity of shelled corn as affected by various drying temperatures. Corn at initial moisture contents of 35 and 54% db was dried at temperatures of 21, 49, 77, and 103 ^{0}C. The porosity for the high and low initial moisture corn was minimum at 20-24 and 17-21% moisture, respectively, and then increased with further drying. Linear regressions for all their samples showed that kernel density increased during drying. Brusewitz (1975) determined the bulk and kernel densities of barley, corn, grain sorghum, oats, rye, soybeans and wheat rewetted to moisture contents of 15-45% wb. Most of the grains except for the grain sorghum and soybeans were found to display a decrease in bulk density with increasing moisture content up to 30% and then the density increased with the moisture content. The bulk and kernel densities as functions of moisture content were fit to a second and a first degree polynomial, respectively. Hao (1992) reported that the bulk densities of wheat at moisture contents of 9, 12, and 16% were 824, 797, and 781 kg/m^3, respectively.

High bulk density implies low volume per unit mass. Changes in in-bin bulk

density during drying or wetting are reflected by bulk contracting or expanding. Sanderson (1986) reported that in a wheat drying experiment, the initial moisture content was approximately 19.0%, the final was 12.5%, and the decrease of bed depth was 11.0% (range 9.4-12.0%). In another wheat drying experiment, the initial moisture content was approximately 18.0%, the final was 8.4%, and the mean bed depth decrease was 12.0% (range 8.5-13.8%). Sanderson et al. (1988) showed that the reduction in bulk volume ranged between 21% when drying 25% moisture content wheat to 13% with near-ambient air, and 9% when drying 18% wheat to 13%. Zhou (1989a) observed that drying barley with near-ambient air from 19.5% to 11.7% moisture content, bulk shrinkage was up to 14.2% of initial volume. Both Sanderson (1988) and Zhou (1989b) tried to record grain bulk expansion during wetting. Unfortunately, no measurable bulk expansion was observed due to the deformation of the cardboard bin walls. After an extensive literature review, Mohsenin (1986) claimed that for food grains, "as the moisture content increases, the molecular attraction becomes smaller and there is a volume increase which is roughly equal to the volume of water added."

It has also been found that bulk density is influenced by pressures. (Clower et al. 1973; Loewer et al. 1977; Thompson and Ross 1983). Clower et al. (1973) studied the effects of vertical pressure on the bulk density of soybean meal, corn meal, sugar beet pulp, and wheat. They found that the functional relationship of bulk density and vertical pressure for all the four granular materials were accurately described by parabolic curves. Loewer et al. (1977) determined the influence of vertical pressure, moisture, and particle size on the bulk density of ground shelled corn. Their results showed that vertical

pressure significantly affected bulk density. Thompson and Ross (1983) measured the bulk density of wheat as a function of moisture content and vertical pressure. The two parameters were allowed to vary over a range of 8 to 24% and 0 to 173 kPa, respectively. Bulk density decreased with higher moisture content at zero pressure. For moisture contents between 8% and 12% wb, a change in bulk density of only 64.2 kg/m^3 was observed over the total range of overburden pressures. Fifty percent of the total change was a result of the rearrangement of the particles in the test apparatus. At moisture contents of 16 and 20%, a total change in bulk density of 112.4 to 160.5 kg/m^3 was noted. The rearrangement of the particles caused only 33 to 40% of the total change and the rest was due to the deformation of grain kernels. For a moisture content of 24%, the particles displayed higher elasticity. The recorded total change in bulk density was 321 kg/m^3. The portion caused by the rearrangement of the particles further reduced to 30%. The remaining change in bulk density was due to the deformation of the particles themselves. The rearrangement of the particles occurred between 0 and 7 KPa.

Filling method affects kernel orientation, consequently affecting the in-bin bulk density. Moysey (1984) studied the effects of grain spreader on grain friction and bin wall pressure. He found that sprinkle fill increased the in-bin bulk density by 7-8%. Muir and Sinha (1988) measured the standard and compacted bulk densities of cereal and oilseed cultivars grown in western Canada. The compacted bulk densities of wheat measured by falling grain from a 2.7 m height were 10-11% greater than their measured standard-bulk-density. Vibration causes grain kernel's rearrangement, leading to a higher bulk density (ASAE 1991).

2.3.2 Friction Coefficient of Grain to Structure Surfaces

Loads exerted on bin walls by stored grain are dependent on interactions between grain and walls. Coefficient of friction, which was originally defined as the proportional constant of the tangential to the normal forces on the contacting surface between two solids in the Coulomb friction law, is commonly used to estimate these interactions. In grain pressure theories, the coefficient of friction correlates the vertical (frictional) force on the bin wall to the lateral (normal) force. There are static coefficient and kinetic (sliding) coefficient. The static coefficient of friction of grain to a structure surface is the ratio of the greatest tangential force not causing grain to move to the normal force acting on the surface through the grain. The kinetic friction coefficient of grain on a structure surface is defined as the ratio of the tangential force required to slide grain over the surface to the normal force pressing the grain against the plane.

Many factors influence the friction coefficient of grain to structure surfaces, including grain moisture content, normal pressure, sliding velocity, surface roughness, the number of trials, surface abrasion, relative displacement between grain and structure, and grain reorientation. Moisture content affects the surface properties of both grain and structure, which in turn influences the coefficient of friction. Brubaker and Pos (1965) experimentally determined the static coefficient of friction for barley, oats, shelled corn, soybeans, and wheat on several wall structural materials over a range of moisture content. The static coefficient of friction increased with the grain moisture content, except on Teflon where surface moisture acted as a lubricant overcoming frictional resistance. When the moisture content of wheat increased from 11.2 to 15.7%, the frictional

coefficient of wheat on galvanised sheet metal increased from 0.10 to 0.33. By pulling a steel blade through grain under pressure, Thompson and Ross (1983) measured the coefficient of friction of wheat on galvanised steel. The coefficient of friction was observed to increase with moisture contents of 8, 12, 16, and 20% wb while it decreased for a moisture content of 24%. Zhang et al. (1994) studied interactions between wheat and a corrugated galvanized steel surface using a modified direct shear apparatus. Their tests were performed at three grain moisture contents (11.9, 14.2, and 17.7% wb) and four pressures (9.73, 34.05, 70.53, and 94.85 kPa). The friction coefficient of wheat on corrugated steel increased with grain moisture content for all pressure levels.

After measuring coefficients of kinetic friction of wheat on various metal surfaces, Snyder et al. (1967) concluded that normal pressure had little effect on coefficient of kinetic friction. However, Thompson and Ross (1983) reported that the friction coefficient of wheat on galvanized steel sheet decreased as the vertical pressure increased from 7 to 172 kPa. Zhang et al. (1994) showed that the coefficient of friction of wheat on a corrugated steel surface decreased with increasing normal pressure over a pressure range from 9.73 to 70.53 kPa and a moisture content range from 11.9 to 17.7%. Vertical shear apparatuses were developed to simulate in-bin friction conditions. Moor et al. (1984) put wheat grain, under pressure, on the outside of three cylinder surfaces. The cylinder was connected to the loading arm of the test machine to measure the friction. They found that the friction coefficients of wheat on corrugated steel and wheat on wheat increased with lateral pressure over a range of 6.90-51.71 kPa. A vertical shear apparatus was developed by Britton and Klassen (1987) to determine grain-structure interactions.

The apparatus comprised a model bin with the wall fixed to the frame of a universal test machine. Wheat contained in the model bin was pressurized using compressed air to simulate in-bin grain stresses. Shear loads were applied to the grain through the loading arm of the test machine. It was observed that friction coefficients of wheat on corrugated wall increased from 0.28 to 0.40 when lateral pressure changed from 10.07 to 53.30 kPa. This result is in agreement with the observation by Moor et al. (1984).

Frictional force is dependent on relative displacement between grain and structure materials (Mahmoud 1979; Zhang et al. 1988). Zhang et al. (1988) proposed an exponential formula, based on experimental results, to correlate the frictional force to the normal force and the relative displacement of wheat for different structural materials. A more comprehensive approach simulating the pre- and post-peak grain-structure frictional behaviour was achieved by Zhang et al. (1991) after conducting experiments to study the frictional behaviour of different grains on a galvanized steel sheet,

When applying the friction concept to corrugated bins, a question arises, which friction should be used, grain-wall friction or grain-grain friction? Moor et al. (1984) found that the shear plane on the corrugated surface developed within the grain confined to the valleys of the corrugations. The location of this shear plane caused simultaneous grain-on-wall and grain-on-grain friction to occur as grain moved along the surface. The frictional coefficient of grain on corrugated surfaces was somewhere between that of grain on smooth wall surfaces and grain-on-grain, but close to the later. This approach was supported by Zhang et al (1994) and tended to support the conclusions of Pieper (1969) and Riembert and Riembert (1980), which suggested that the side wall friction should be

equal to grain-on-grain friction.

2.3.3 Ratio of Lateral to Vertical Pressure

There has been controversy surrounding the determination of the ratio of lateral to vertical pressure. Koenen (1896, cited by Smith and Simmonds 1983) recommended that the Rankine theory for active earth pressure could be borrowed to estimate K, in which K was defined as a function of the internal friction angle ϕ: $K=(1-\sin\phi)/(1+\sin\phi)$. For an internal friction angle of 30^0, this gives a K value of 0.33. Jaky (1948, cited by Moysey 1979) suggested that K should be $1-\sin\phi$, which gives a K value of 0.5 for $\phi=30^0$. Taking the effects of wall friction into account, Moysey (1979) derived two formulas for calculating K adjacent to the bin wall in the active and passive cases by means of Mohr's circles. For the active case, $K=(1-\sin\phi\cos2\theta)/(1+\sin\phi\cos2\theta)$, where θ is the angle between the principal plane and the horizontal direction; for the passive case, $K=(1-\sin^2\phi)/(1+\sin^2\phi)$.

Experimentally measured K varied widely. Early experiments reported by Ketchum (1919) showed K up to 0.6. In Russian experiments, values of 0.68 to 0.74 were obtained for K (Moysey 1979). Canghey et al (1951) reported a K value of 0.6 for wheat and corn. Clower et al. (1973) measured K for four granular materials under different pressures and found that K ranged from 0.30 to 0.67 for wheat. The value of K was found to be essentially independent of vertical pressure. The mean K values for wheat, soybean meal, corn, and sugar beet pulp were 0.52, 0.44, 0.50, and 0.59, respectively. Loewer et al. (1977) developed an empirical equation to calculate K as a function of moisture content and pressure based on their experimental results.

Atewologun and Riskowski (1991) determined K at the bin centre for soybeans using in-mass transducers. They found that for grain depth less than H/D=2.8, K decreased from 0.67 to 0.47 when grain depth increased from 121.9 to 259.1 cm. At the depths about three times the bin diameter (H/D=3.0), K approached a constant value that may be approximated as: $K=(1-\sin\phi)$. The value of K was also found to vary in the radial direction.

2.4 Moisture Induced Loads

Blowing near-ambient air through grain stored in a bin creates a moisture transferring front which travels upwards through the bulk (Dougan 1992) (Fig. 2.1). Moisture transfer between the grain and air takes place in the front. The grain below the front reaches equilibrium with the flowing-by air. When the relative humidity of the air is lower than the ERH of the grain, some of moisture in the grain is evaporated and carried away by the air and thus the grain is being dried. As drying progresses, grain kernels shrink and the grain bed settles down. When the relative humidity of the air is higher than the ERH of the grain, the air adds moisture to the grain and thus the grain is being wetted. During wetting, grain kernels swell. This causes the grain bulk to expand. Both lateral and vertical pressures increase. The grain bulk expansion is limited laterally by the bin wall and vertical by the floor. Therefore, when the vertical pressure in the lower section of the bin is high enough to overcome the gravity force of the grain mass and the friction between the wall and grain, the grain bulk moves upward.

Dale and Robinson (1954) measured moisture induced pressures in a model bin 5 ft (1.5 m) high and 18 in (0.46 m) in diameter. The bin was filled with shelled corn

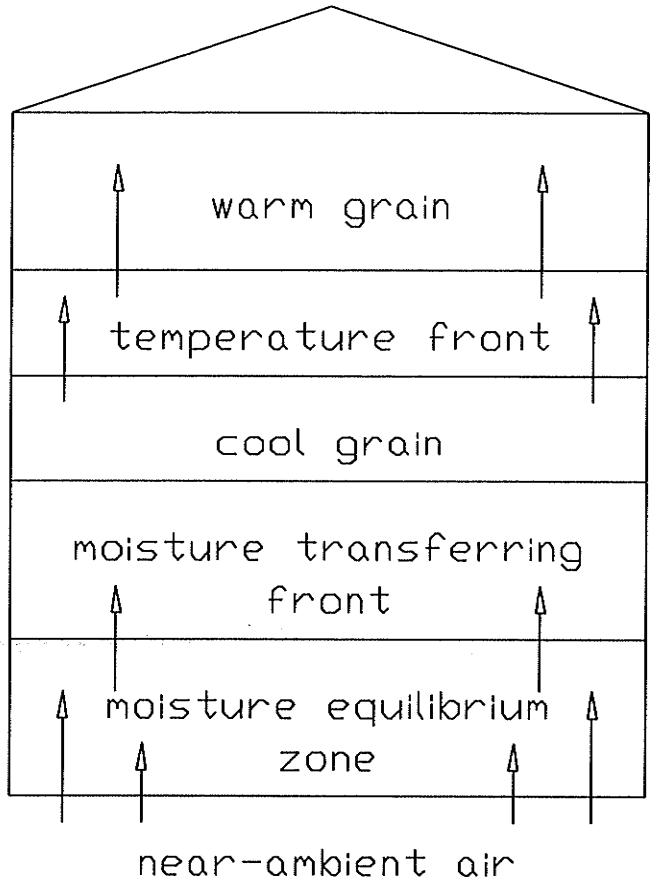

Fig. 2.1 Blowing near-ambient air through grain bulk creates a moisture transferring front and a temperature front.

and air at an average relative humidity of 78% was blown through the grain bulk to wet the grain. When the grain moisture increased from an initial of 13.2 to an average of 15.0% wb, lateral pressure near the bin floor increased from 0.52 (3.59) to 2.00 psi (13.80 kPa), or 3.8 times. To simulate flood conditions, shelled corn at 12.5% moisture in the bin was completely soaked in water for a period of 10 minutes; the excess water was then drained from the bin. They observed that the maximum pressures developed in approximately two hours. The maximum lateral pressure was approximately ten times the pressure of dry grain at that depth as predicted by Jassen's equation. Blight (1986) determined swelling pressure of several grains and oilseeds using an oedometer. The specimen of grain was contained in the oedometer chamber 42 mm high and 70 mm in diameter and loaded vertically with a series of pressure increments up to 64 kPa. The loaded grain was inundated with water and then drained to simulate the ingress of rain. The highest pressure increase observed was for gain sorghum: from 28 to 115 kPa, or 4 times. Britton et al. (1993) measured vertical forces on the wall of a model bin during the wetting of stored grain. Their bin was 1.5 m high and 1.0 m in diameter, filled with wheat at an initial moisture content of 10% wb. When the grain bulk was wetted by blowing humidified air for about 900 min., the vertical (frictional) force on the wall was completely balanced by the upward lifting force of grain swelling. The swelling force eventually uplifted the wall from the bin floor.

Zhang and Britton (1994) developed the first model to predict moisture induced loads in grain bins. Volumetric increase of a wetted grain kernel was assumed to be equal to the volume of water absorbed by the kernel. The volumetric strain of the grain

bulk due to moisture changes was calculated from swelling of individual grain kernels. Using typical material property parameters for shelled corn, their model predicted a hygroscopic overpressure factor of 9 for a moisture increase of 4% db. Based on empirical equations describing correlations between kernel density and moisture content for grains, Zhang et al. (1995) derived another mathematical formula for calculating hygroscopic pressures in grain storage structures. For a hypothetical bin 10 m high and 5 m in diameter subject to a moisture increase of 10% db, predicted pressures were 7.3, 6.2, 4.8, and 4.4 times the static pressures for wheat, corn, barley, and oats, respectively.

Chapter 3

OBJECTIVES

From the literature cited in the above review, it is clear that the study of grain bin loads is a complex subject. Even when analyzing static loads, many factors need to be considered. But many of these factors are still little understood, and their effects on static loads have not been precisely defined. Most physical properties of grain change with grain moisture. Although research has showed that increase in grain moisture can induce extremely high grain pressures, more work is needed to investigate the nature and magnitude of bin loads during drying and wetting of stored grain. The specific objectives of this study were to:

1) compare measured static pressures with Janssen's predictions;

2) measure structural loads in a model grain bin during drying and wetting of the stored grain; and

3) determine the ratio of lateral to vertical pressure during the processes.

Chapter 4

EXPERIMENTAL METHODOLOGY

4.1 Test System

A model bin system located in the Department of Biosystems Engineering, University of Manitoba was used to conduct the experiment. The system consisted of a model bin, force and pressure transducers, a data acquisition unit, an air supply system and a grain handling system (Fig. 4.1).

4.1.1 Model Bin

A solid wooden deck placed on the top of a steel triangle provided a base table to support a model bin. The steel triangle was suspended by three 12 mm steel rods located 120^0 apart, each of which is connected to a steel frame through a load transducer. These load transducers measured the mass of grain in the bin. The bin, 0.96 m in diameter and 1.57 m high, was constructed from 0.97 mm thick corrugated galvanized steel sheets. the bin was supported on the base table through three load transducers located 120^0 apart along the mounting ring of the wall. These three wall load transducers sensed the resultant vertical force on the wall. There was a plenum (320 mm high) between the bin and the base table. A 1.6 mm punched steel sheet installed on the top of the plenum was used as the bin floor to support the grain and to allow air to pass through. Between the wall mounting ring and plenum, there was a 35 mm high circular sealing ring. The diameter of the ring was 15 mm smaller than the inner diameter of the wall. The lower side of the ring was connected to the plenum and its upper side stretched slightly into the bin wall. The bin wall was skirted inside near the bottom with a piece

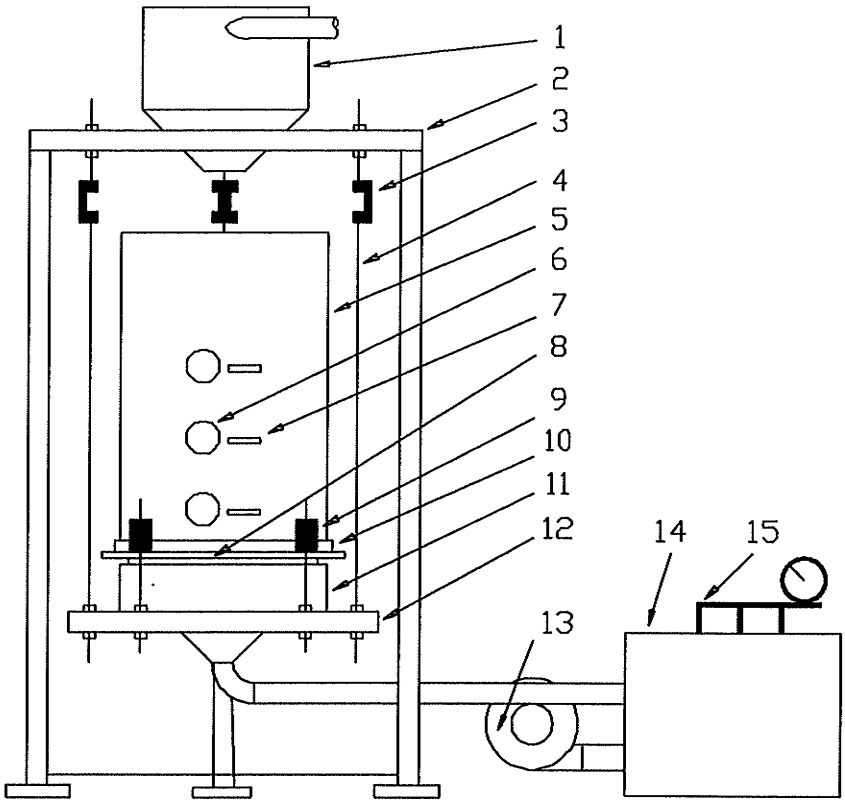

Fig. 4.1 Schematics of the test bin system. 1-surge bin; 2-steel frame; 3-floor load transducer; 4-steel rod; 5-model bin wall; 6-horizontal pressure sensor; 7-vertical pressure sensor; 8-sealing ring; 9-wall load transducer; 10-bin wall mounting ring; 11-plenum; 12-base table; 13-fan; 14-humidity chamber; 15-spray nozzle.

of plastic membrane extending into the sealing ring to keep the grain and air from leaking. The membrane was thin and flexible. It could not transfer any vertical load between the bin wall and plenum.

4.1.2 Force and Pressure Transducers

Both the floor and wall load transducers were C-clamp type force transducers and were calibrated using dead weights. All calibration equations were linear, with R^2>99.9% (APPENDIX A). Each floor load transducer had a load design capacity of 5.0 kN and was calibrated from 0 to 3.88 kN. As both upward and downward loads were induced on the wall during the drying and wetting of stored grain, the wall load transducers were designed to measure loads on the wall in both directions (Fig. 4.2). The load design capacity of each wall load transducer was 2.5 kN. The load calibration range was from 0 to 1.96 kN.

Six diaphragm sensors were used to measure grain pressures in this study. Senors, with a diaphragm 0.65 mm thick and 60 mm in diameter, were carefully machined out of aluminum disks (Fig. 4.3). When a normal pressure is applied to the diaphragm, the maximum radial tension strain occurs in the central area of the diaphragm, and the maximum radial compression strain occurs at the edge. Four strain gages were mounted on the diaphragm, two at the centre and the other two near the edge to achieve the maximum sensitivity. The four strain gages were connected into a full bridge electric circuit. The design of pressure sensors was detailed in APPENDIX B. All the diaphragm pressure sensors were calibrated using dead weights from 0 to 32 kPa. The pressure-strain relationship for all the sensors was linear, with R^2>99.6%. During calibrating, a

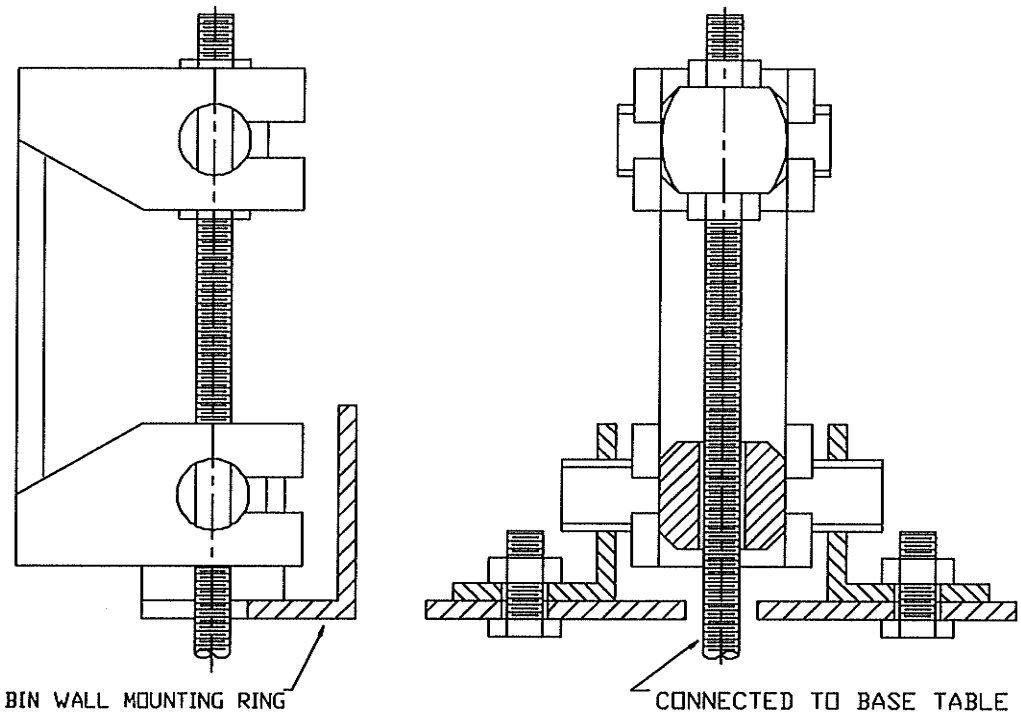

Fig. 4.2 Schematics of load transducer

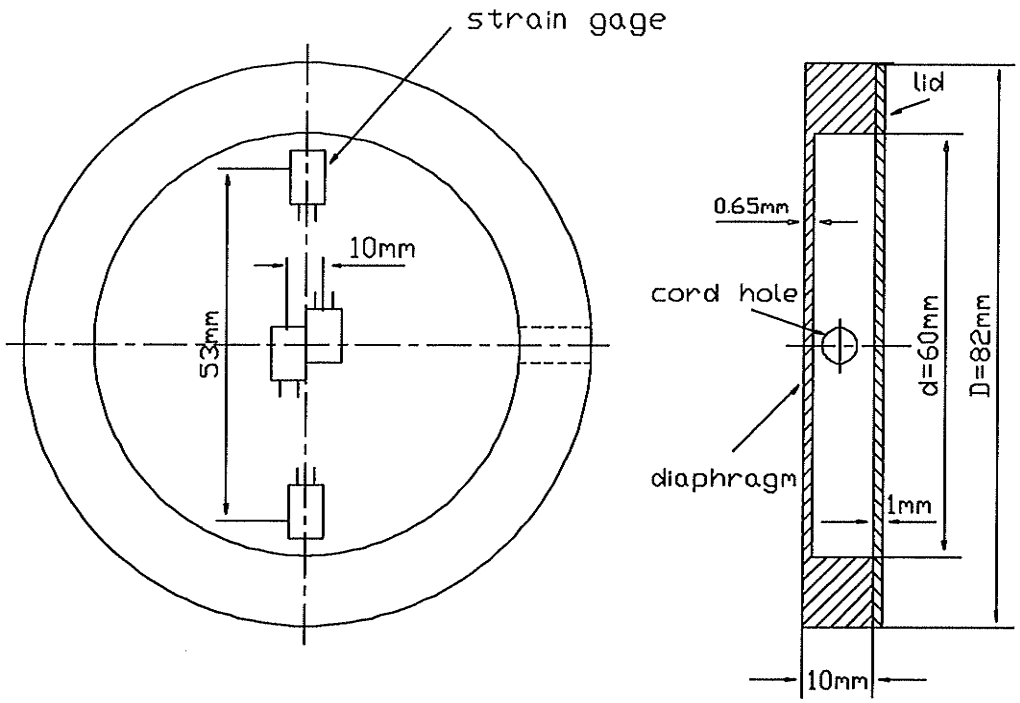

Fig. 4.3 Schematics of pressure sensor.

plastic cylinder, 60 mm in diameter and 50 mm high, was centred on the diaphragm to hold wheat grain (Fig. 4.4). Before the cylinder was filled with grain, two 1.5 mm thick metal shims, were inserted between the cylinder and sensor as a spacer. The grain filled in the cylinder was consolidated by shaking the cylinder for half a minute by hand and excess grain was struck off with a rod. A steel disk, 56 mm in diameter and 5 mm thick, was placed on the top grain surface to transmit the dead weights to the grain. The shims were taken out before loading dead weights to create a clearance between the bottom of the cylinder and the diaphragm so that the gravity of dead weights was transmitted to the sensor completely through the grain.

The six pressure sensors were installed in three pairs in the bin. Each pair were fixed on a horizontal 90^0 angle steel bracket with one sensor measuring vertical pressure and the other measuring the lateral. The horizontal distance between the central points of the sensors in each pair was 110 mm. All three pairs of sensors were placed in the grain, 100 mm radially from the outer extreme of the bin wall and they were placed 384 mm apart vertically, starting 140 mm from the bin floor (Fig. 4.1). Before the bin was filled, each pair of the sensors was held in position by two steel rods stretching into the angle steel bracket from a supporting frame fixed on the bin wall. The rods were removed once the bin was filled so that sensors could "float" with grain as it contracted or expanded.

To monitor the drying front in the bin during the experiment, four thermocouples were installed in the grain mass. They were placed 20 mm radically from the bin wall and 384 mm apart vertically starting 140 mm from the bin floor. Two other

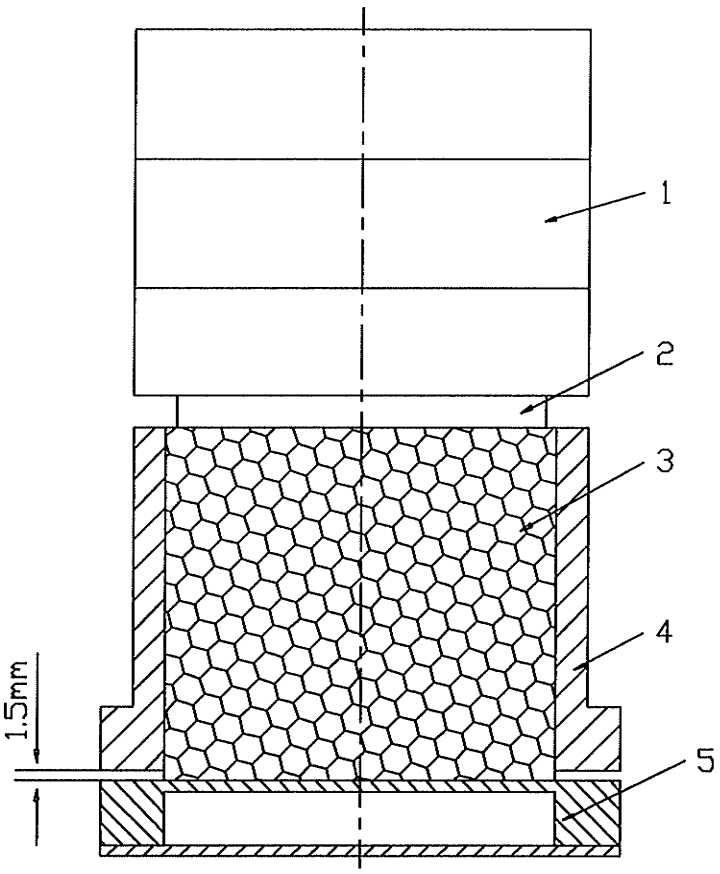

Fig. 4.4 Schematics of calibration set-up for pressure sensor. 1-dead weight; 2-steel disk; 3-wheat grain; 4-plastic cylinder; 5-pressure sensor.

themocouples were installed to measure air temperature in the plenum and ambient air temperature.

4.1.3 Data Acquisition System

Strain readings from force and pressure transducers and temperature readings from thermocouples were taken by using a HP 8352A data acquisition unit connected to a microcomputer. The computer provided both data acquisition unit control and data storage. The height of grain surface was measured by using a sliding gage mounted on the top edge of the wall.

4.1.4 Air Supply System

An air supply system included a centrifugal fan, a humidity chamber, and some ducts. The fan with a 90 mm (in diameter) outlet was driven at a speed of 5400 rpm by a 0.5 hp electric motor. The air flow rate was 50 L/s, at a pressure of 2.5 kPa. The humidity chamber was a 0.5 x 0.5 x 1.0 m wooden box. Three sprayer nozzles were installed in the chamber and connected to a pressure regulator. Water at a pressure of 380 ± 35 kPa was injected into the chamber to humidify the flowing air to a relative humidity of $80\pm10\%$ during wetting. In the drying processes, the nozzles were turned off.

4.1.5 Grain Handling System

A circular surge bin connected to a pneumatic conveyor was mounted on the top of the steel frame to provide consistent central filling. The outlet of the surge bin was 2.3 m above the model bin floor. The surge bin was filled with grain by the pneumatic conveyor and then the grain was discharged to the model bin.

4.2 Materials

Freshly-harvested hard red spring wheat, which had been stored in a ventilated bin on a farm for several days, was used in the study. The initial physical properties of the wheat are showed in Table 4.1 and the physical properties of the grain at different moisture contents are described in Table 4.2. Wheat was sampled for initial property measurements just before the test started. Physical properties of wheat at different moisture contents were determined by using grain samples obtained after being dried. These samples had a moisture content of 8.0%. Water was then added to the samples to achieve higher moisture contents. The grain samples were thoroughly mixed and stored in airtight plastic bags for at least 3 days at room temperature (22 ± 2^{0}C) before physical properties were measured. All moisture contents were determined by the oven dry method specified by ASAE (1990) and expressed on a dry basis.

Bulk density was measured according to the method specified by the Canadian Grain Commission. The grain was placed in a cone having a top diameter of 225 mm, a bottom diameter of 38 mm, and a height of 160 mm. The bottom of the cone was 45 mm above the top of a cup, 90 mm in diameter and 79 mm deep. When the flat slide gate on the bottom of the cone was open, the grain dropped freely into the centre of the cup. The excess grain on the top of the cup was struck off with a rod and the mass of grain in the cup was measured. In-bin bulk density represents the average value of bulk density of grain in the bin in this thesis. It was determined as the mass of grain in the bin divided by the volume occupied by the grain and intergranular space.

To determine kernel density, the volume occupied by a known mass of kernels

Table 4.1 Initial physical properties of wheat used in the study

Moisture content, %, db	14.1*(0.2)**
Bulk density, kg/m^3	719.5(1.5)
Kernel density, kg/m^3	1408.0(2.1)
Porosity, %	49.1(0.1)
In-bin bulk density, kg/m^3	794
In-bin porosity, %	43.7
Emptying angle of repose, degree	31.0(0.5)

* means from three measurements.
** standard deviations.

Table 4.2 Physical properties of wheat at different moisture contents

Moisture content %, db	Bulk density kg/m^3	Kernel density kg/m^3	Porosity %	Emptying angle of repose degree
8.0*(0.0)**	777.2(0.5)	1445.3(4.6)	46.2(0.2)	26.0(0.4)
9.4(0.1)	760.0(1.1)	1436.3(1.3)	47.1(0.1)	27.6(0.4)
10.9(0.1)	741.9(2.5)	1427.5(1.0)	48.0(0.1)	28.9(0.6)
12.4(0.3)	732.9(2.3)	1420.0(2.5)	48.4(0.1)	30.3(0.5)
14.2(0.2)	717.5(1.9)	1406.9(2.2)	49.0(0.1)	31.0(0.5)
15.5(0.1)	708.5(2.0)	1401.9(6.4)	49.4(0.1)	31.5(0.5)
17.1(0.1)	701.1(1.4)	1388.7(1.3)	49.5(0.1)	31.5(0.5)
19.1(0.1)	692.1(2.3)	1360.9(5.5)	49.1(0.3)	33.6(0.6)

* means from three measurements.
** standard deviations.

was determined with an air comparison pycnometer (Model 930, Beckman Instruments Inc., CA). Porosity was calculated using standard bulk density and kernel density. In-bin porosity was computed using in-bin bulk density and kernel density.

Emptying angle of repose is the angle included between the horizontal and the sloped upper surface of a grain pile created when the grain is allowed to flow out through an opening at the bottom of the pile. Emptying angle of repose was measured with a cubic box of 306 x 306 x 306 mm. The box was filled with grain to a depth of about 200 mm. The grain was then allowed to flow out through a 40-mm-diameter opening at the centre of the bottom. The emptying angle was calculated from measurements of grain left in the box.

4.3 Experimental Procedures

The test bin was centrally filled with wheat dropping freely from the surge bin. When grain surface was about 10 cm over the pressure sensors, the filling was paused shortly and the supporting frame was taken off from the angle steel bracket so that the pressure sensors could float with grain mass during expansion and contraction. Strain readings and grain surface height measurements were taken as initial (or static) values before the fan was turned on. The grain was first dried and then was subjected to three wetting-drying cycles continually. When grain moisture became relatively constant during a cycle, test was switched to the next process.

During the experiment, strain readings and temperature readings were taken every 30 minutes. The height of grain surface were measured about every 24 hours. Raw strain data were converted into weights, forces, and pressures using the sensor calibration

equations. The average moisture content of grain, during wetting and drying was determined as:

$$MC_a = \frac{(1 + MC_i)M_c}{M_i} - 1 \qquad (5)$$

where MC_a = average moisture content during drying, (%, db);

MC_i = initial moisture content of grain, (%, db);

M_c = current mass of grain, (kg);

M_i = initial mass of grain, (kg).

Chapter 5

RESULTS AND DISCUSSION

5.1 Temperatures and Grain Bulk Volume

Typical curves of recorded temperatures of the ambient air, air in the plenum, and grain during wetting and drying are shown in Fig. 5.1 and Fig. 5.2. During wetting, the grain temperature followed that of the ambient air. The same trend was observed for the drying processes. However, the grain temperature and the ambient air temperature never became the same. In both drying and wetting processes, temperature differences between the bottom and middle levels were always greater than those between the middle and top levels. This indicates that the difference in the grain moisture content between the lower two levels was greater than that between the upper two levels as moisture transfer follows temperature transfer during drying.

Recorded grain surface heights were converted into bulk volume changes. Changes in bulk volume and AMC (average moisture content) of the grain during the drying and wetting periods are summarized in Table 5.1. At the end of each drying cycle, the bulk volume of the grain decreased although there was little difference in final average moisture contents of the grain at the end of drying cycles. This volume decrease became less significant as the number of cycles increased. It follows that the change in bulk volume for 1% of moisture decrease was greater in an earlier drying cycle than in a subsequent drying cycle. It was believed that the decreases in bulk volumes were mainly caused by further reorientation of grain kernels. Most reorientation took place during the first cycle and the degree of reorientation decreased as the experiment

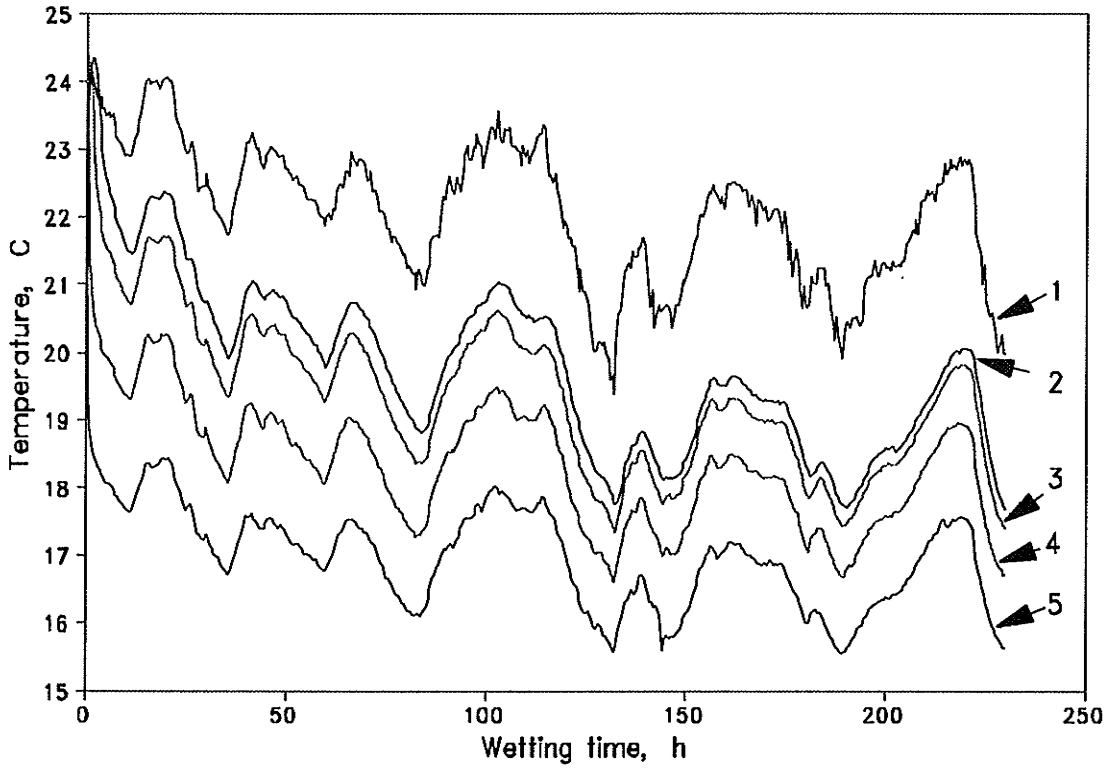

Fig. 5.1 Temperature change during the second wetting cycle. 1-temperature of ambient air; 2-temperature at top level in the bin; 3-temperature at middle level; 4-temperature at bottom level; 5-temperature of humidified air in plenum.

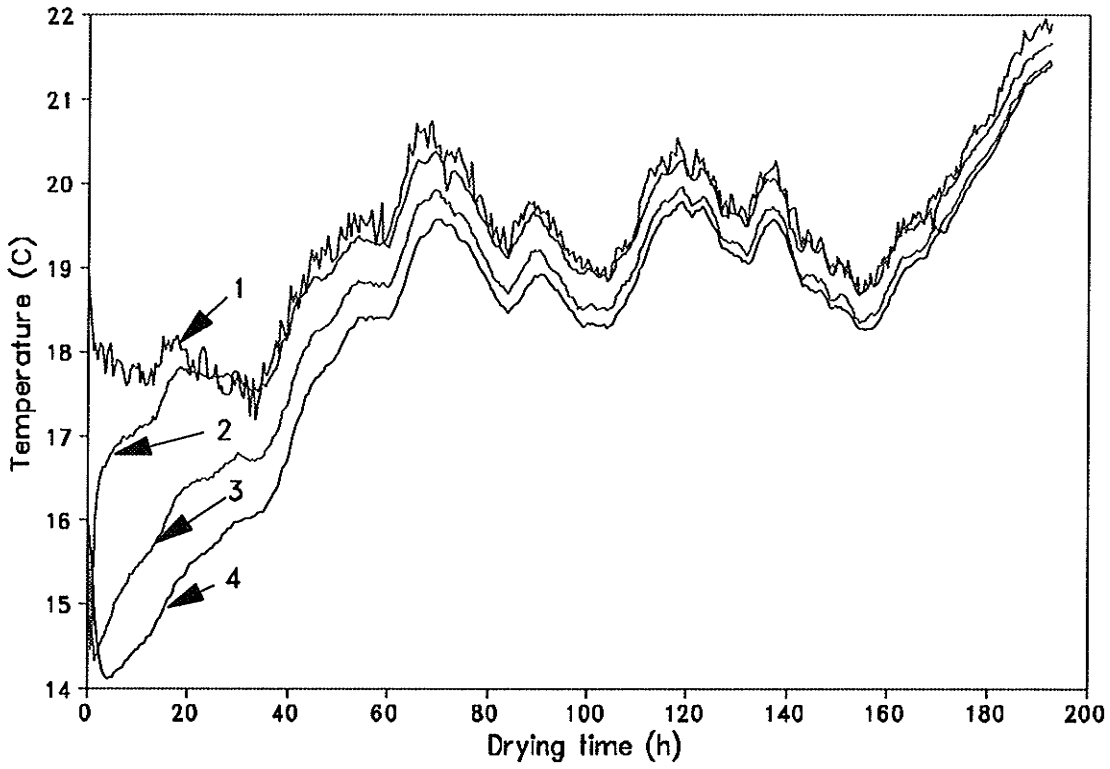

Fig. 5.2 Temperature change during the third drying cycle. 1-temperature of ambient air; 2-temperature at bottom level; 3-temperature at middle level; 4-temperature at top level.

progressed. The bulk volume increased in a later wetting cycle than in an earlier one. In contrast, this implies that there existed less porosity in the grain bulk in a later wetting cycle. At the end of the last two drying cycles, the values of grain bulk volume were almost the same. This implies that reorientation of grain kernels had reached the limit after two cycles.

Table 5.1 Changes in bulk volume and AMC of the grain

	DC1	WC1	DC2	WC2	DC3	WC3	DC4
AMC (%db)	14.1*	8.7	19.6	9.5	17.5	9.3	16.5
	11.0**	19.7	9.2	17.6	9.4	17.0	9.2
ABV (L)	120.2*	110.8	113.3	105.8	108.4	103.6	106.7
	112.5**	113.3	105.8	108.4	103.6	106.7	103.7
BV (%)	100.0*	92.2	94.3	88.0	90.2	86.2	88.8
	93.6**	94.3	88.0	90.2	86.2	88.8	86.3
BVC (%)	-2.06	+0.19	-0.61	+0.27	-0.49	+0.34	-0.34
ABD (kg/m^3)	794.0*	820.4	882.5	865.8	906.4	882.3	912.8
	820.0**	883.2	863.5	907.2	883.1	916.8	880.5

Note:
1. WC = wetting cycle; DC = drying cycle.
2. The experiment stopped for one week between DC1 and WC1.
3. ABV = actual bulk volume of the grain in the bin; BV = bulk volume of the grain in the bin; BVC = bulk volume change of the grain in the bin for 1% AMC change; ABD = average bulk density of the grain in the bin. Both BV and BVC are in percentage of the initial bulk volume. Negative means decrease; positive means increase.
4. * and ** are values at the beginning and end of a process, respectively.

5.2 Static Loads

Bin loads measured before the drying and wetting started are considered as static loads. The static vertical and lateral pressures were in reasonable agreement with Janssen's predictions (Fig. 5.3). The initial bulk density of 794 kg/m^3, the grain-wall friction of 0.4, and the average measured K of 0.47 were used in Janssen's prediction. The measured static vertical forces on the floor and wall were 5.63 kN and 3.72 kN and they represented 60% and 40% of the total grain weight, respectively. The vertical load carried by the bin wall in the corrugated bin was two times as high as that in a smooth bin wall of the same size (Pokrant 1987). The difference is due to greater grain-wall friction in the corrugated bin. When the measured vertical force on the floor was used to compute the average vertical pressure at the bin bottom level, a value of 7.12 kPa was obtained, which is 8.6% higher than the measured vertical pressure. This indicates that the vertical pressure is not constant across the bin diameter. The measured vertical pressure close to the wall was lower than the average due to wall friction. The vertical wall load predicted by $F = (wgY-0.8V)R$, was 1.71 kN/m, or a total vertical wall load of 1.71 x C=5.16kN, where C is the circumference of the bin. The predicted vertical wall load is 38.6% greater than the measured value. The static lateral to vertical pressure ratio (K) at the top, middle, and bottom levels were 0.48, 0.47, and 0.46, respectively. By using the emptying angle of repose to approximate the angle of internal friction (ϕ), the Rankine equation $((1-\sin\phi)/(1+\sin\phi))$ predicts a K of 0.32, which is 68% of the average measured K. The formula $(1-\sin\phi)$ suggested by Jaky (1948, cited by Moysey 1979) gives a K value of 0.48, which is almost the same as the average measured K.

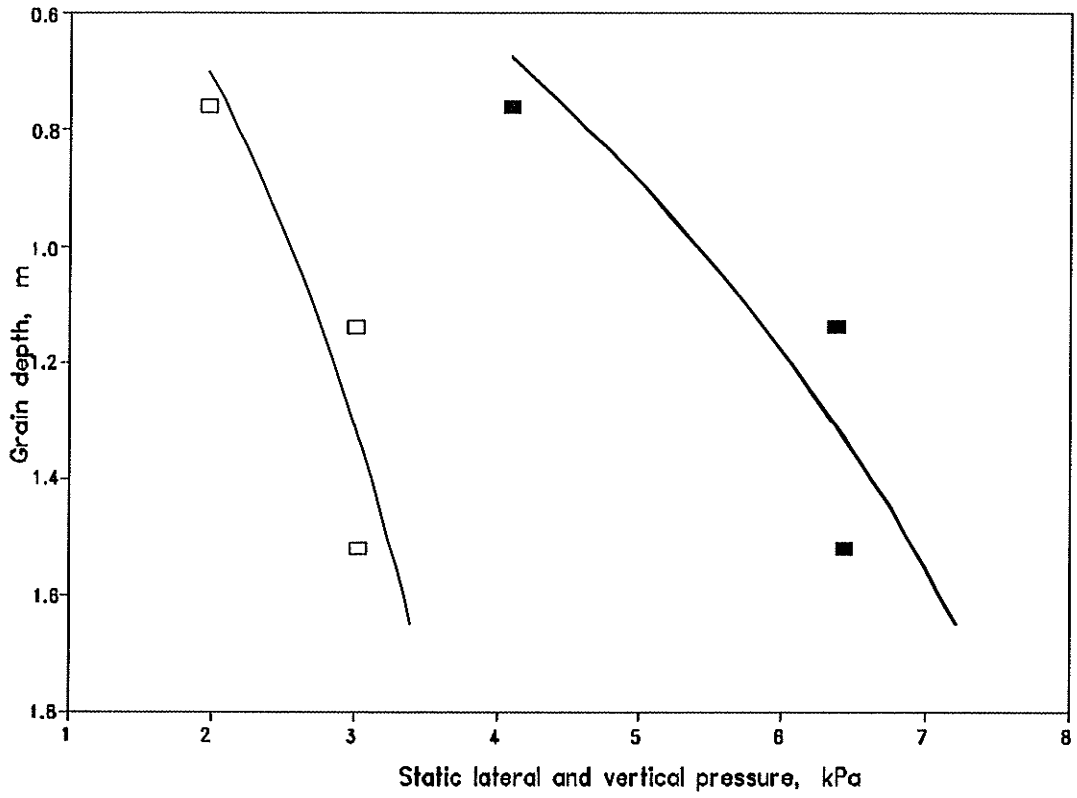

Fig. 5.3 Comparison of measured lateral and vertical pressures with Janssen's predictions under static conditions.

5.3 Bin Loads during Initial Drying

During the initial drying period (DC1), the grain was dried from a moisture content of 14.1% to an average (AMC) of 11.0%, db. The total grain mass decreased by 2.7% due to moisture loss. The vertical force on the floor increased from 5.63 to 5.74 kN, or 2.0%; the vertical force on the wall decreased from 3.72 to 3.37 kN, or 9.4 % (Fig. 5.4). Assuming this 2.7 % decrease in total grain mass alone cause a 2.7% decrease in both vertical forces on the floor and wall, the increase in vertical floor load and the decrease in vertical wall load due to changes in material properties were computed to be 4.7% and 6.7%, respectively. Therefore, load changes were resulted from decreases in bulk density, as well as in the grain internal friction and grain-wall friction. The vertical floor load dropped slightly and the vertical wall load rose slightly at the beginning of drying. That was because that the grain bulk partly lost its support due to the shrinkage of grain kernels at the bottom, which caused a shifting of vertical load from the bin floor to the wall. Another two sudden load shiftings were observed during the experiment (Fig. 5.4) because of the sudden collapses of arches in the grain as the grain bulk contracted.

Both lateral and vertical pressures at the top level fluctuated most (Fig. 5.5). The reason was unclear. Lateral pressures at the middle and bottom levels remained almost constant (Figs. 5.6 and 5.7). This implied that the effects of decreases in grain internal friction and grain mass on lateral pressure almost cancelled out each other, as decreases in grain internal friction cause increases in lateral pressure, whereas, decreases in grain mass result in decreases in loads. Vertical pressures at both middle and bottom levels increased during the first 15 hours and then remained almost constant. Increases in

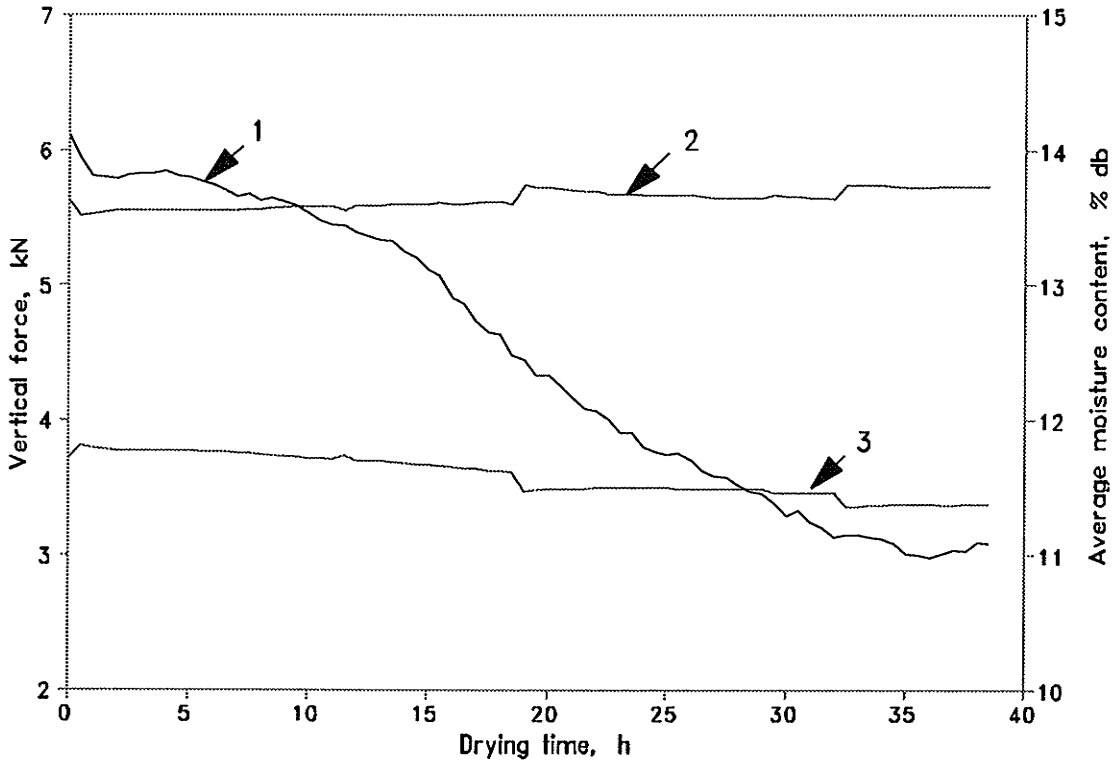

Fig. 5.4 Variations of vertical forces on the bin floor and wall during the first drying period. 1-average moisture content of grain; 2-vertical force on floor; 3-vertical force on wall.

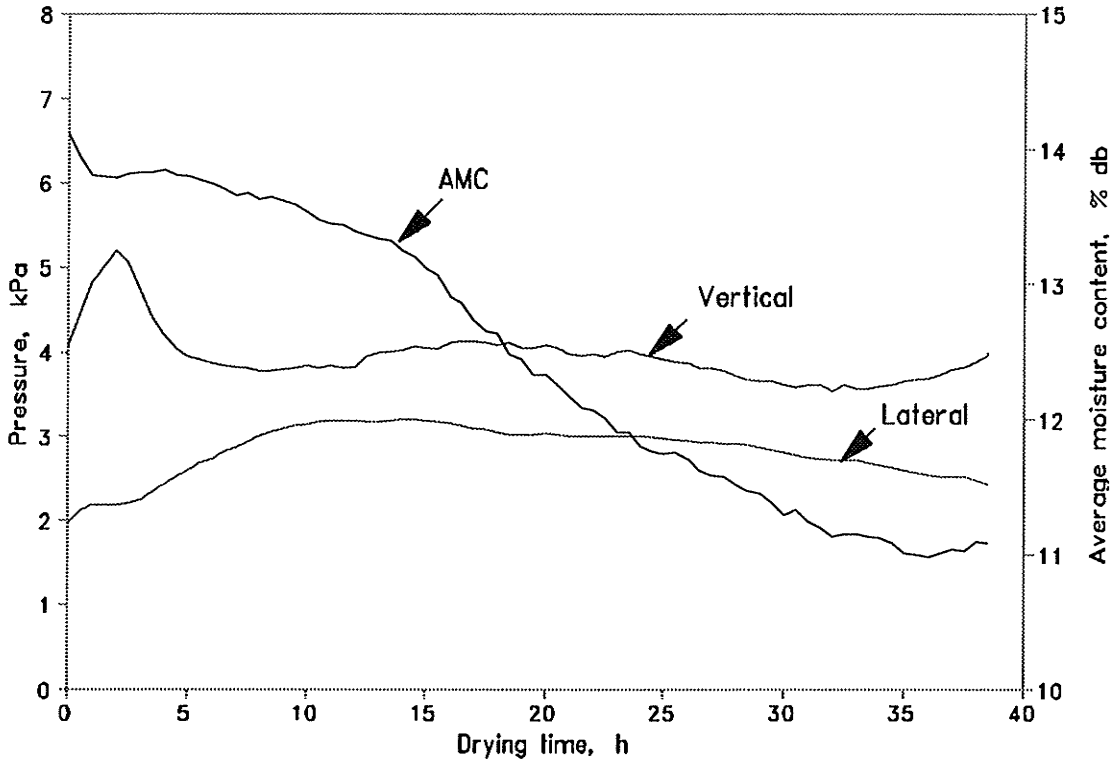

Fig. 5.5 Variations of vertical and lateral pressures at the top level during the first drying cycle.

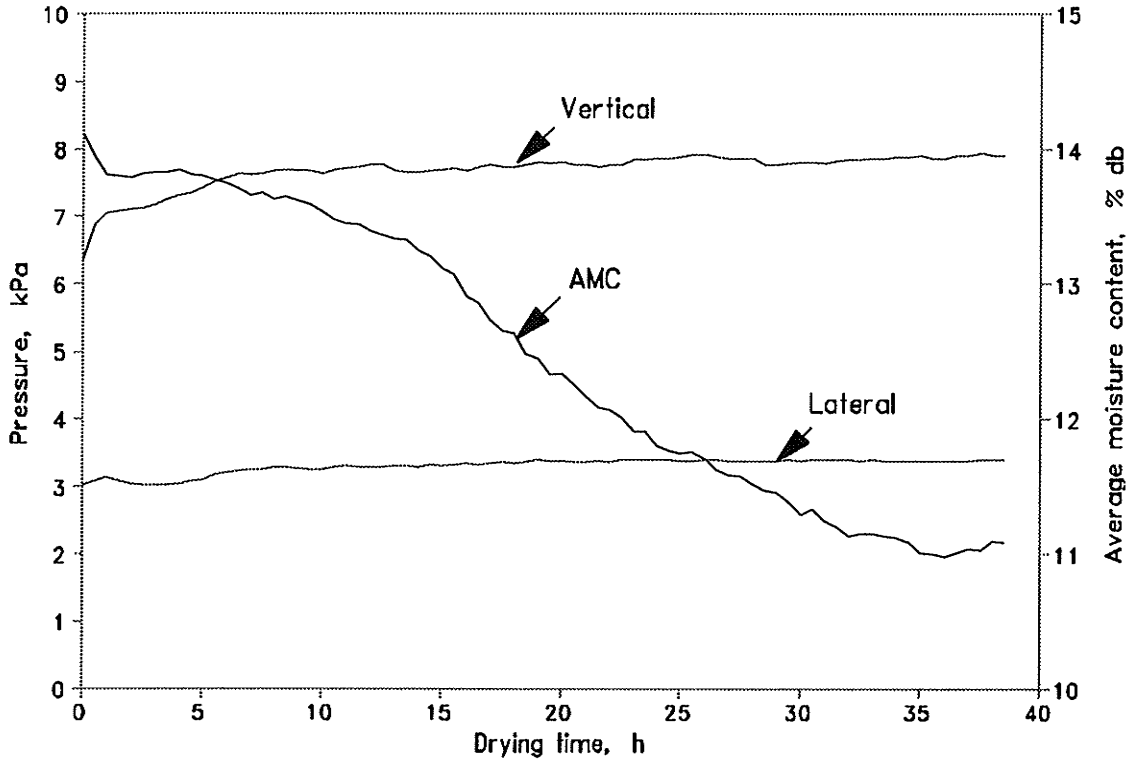

Fig. 5.6 Variations of vertical and lateral pressures at the middle level during the first drying cycle.

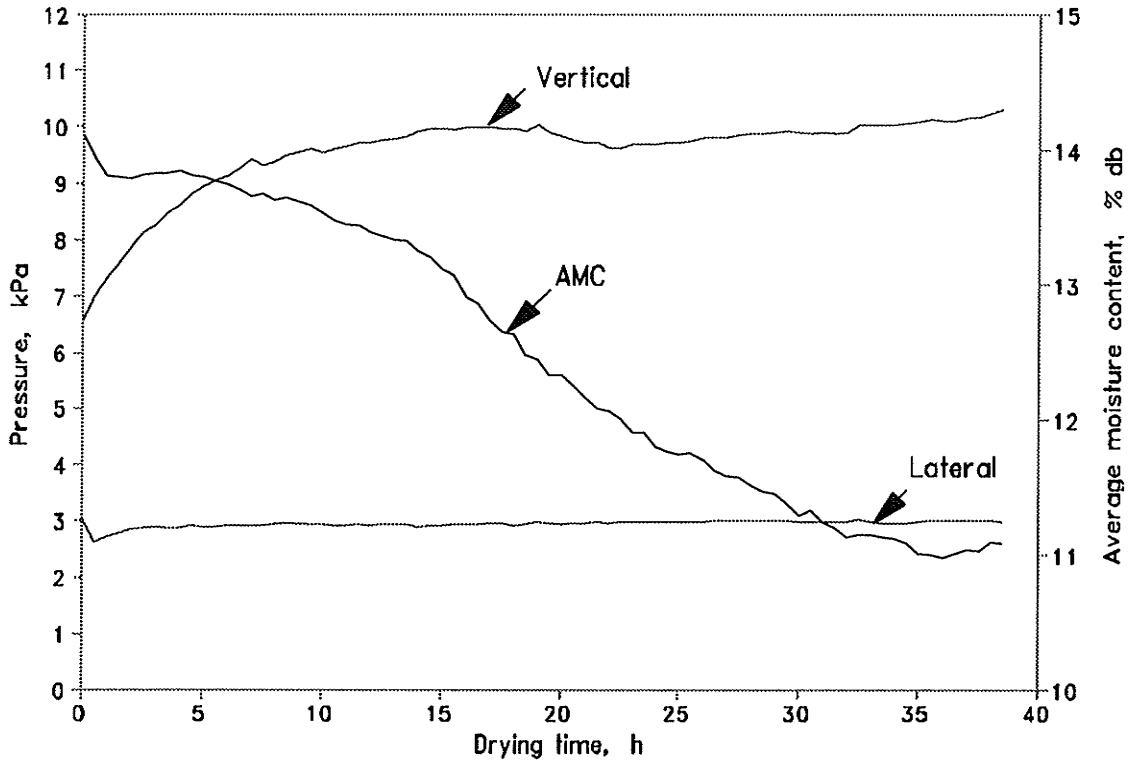

Fig. 5.7 Variations of vertical and lateral pressures at the bottom level during the first drying cycle.

vertical pressure were attributed to decreases in internal friction and grain-wall friction as the grain was dried. The overall increases in vertical pressure were from 6.56 to 10.11 kPa at the bottom level, and 6.37 to 7.87 kPa at the middle level. A greater increase in vertical pressure occurred at the lower level because the grain moisture decreased more at the lower section of the bin. At the middle and bottom levels, the lateral to vertical pressure ratios varied between 0.22 and 0.47. At the top level, K fluctuated in a range from 0.30 to 0.87.

5.4 Bin Loads during Wetting

5.4.1 Starting State of the Wetting Cycles

Although differences in starting values of the AMC between wetting cycles were small (within 0.8%), there existed some differences in the starting values of vertical loads on the floor and wall (Table 5.2). The starting values of vertical forces on the floor and wall were 5.63 and 3.26 kN for the first wetting cycle, 6.32 and 2.64 kN for the second, 6.48 and 2.47 kN for the third, respectively. The vertical floor load increased and wall load decreased with the number of drying-wetting cycles. This was probably attributed to the fact that the grain became more compacted every time a drying-wetting cycle went though. As the drying and wetting cycles continued, grain bulk contraction and expansion tended to reorient grain kernels to a more stable position, thus the strength of the grain bulk increased. The increased bulk strength caused load to shift from wall to floor. The average bulk densities of the grain were 820, 866, and 882 kg/m^3 at the beginning of the first, second, and third wetting cycles, respectively (Table 5.1). The measured variations of starting vertical and lateral pressures (Table 5.3) were generally consistent with those

of the vertical loads. Higher vertical and lower lateral pressures were observed at the beginning of a later wetting cycle. Differences in the starting vertical loads between the second and third wetting cycles were smaller than those between the first two wetting cycles. That might be mainly attributed to a reduced degree of reorientation, as grain was subjected to more drying-wetting cycles.

5.4.2 Vertical Forces on the Floor and Wall

As the grain was wetted, vertical force on the floor increased and an upward lifting force caused by grain bulk expansion reduced the downward vertical force on the wall to zero and then reversed frictional force on the wall. The greatest increases in vertical forces on the bin floor and wall occurred during the third wetting cycle. The vertical force on the floor increased from 6.48 to 15.43 kN, or a net of 8.95 kN for an

Table 5.2 Vertical forces on the bin floor and wall during wetting cycles

		WC 1	WC 2	WC 3
AMC,% db		8.7—19.7	9.5—16.2	9.3—15.4
VF_f (kN)	starting	5.63	6.32	6.48
	peak	14.28	14.01	15.43
	net increase	8.65	7.69	8.95
	peak/starting	2.5	2.2	2.4
	peak/static	2.5	2.5	2.7
VF_w (kN)	starting	3.27	2.64	2.47
	peak	-4.47*	-4.50	-5.98
	net change	-7.74	-7.14	-8.45
	peak/starting	1.4	1.7	2.4
	peak/static	1.2	1.2	1.6

Note: 1. VF_f = vertical force on the floor; VF_w = vertical force on the wall.
2. * negative means upward force.

5.3 Vertical and lateral pressures during wetting cycles

		WC 1	WC 2	WC 3
AMC (% db)		8.7-19.7	9.5-16.2	9.3-15.4
VP_T (kPa)	starting	3.03	4.20	4.46
	peak	20.22	17.05	19.06
	net increase	17.19	12.85	14.60
	peak/static	5.0	4.2	4.7
LP_T (kPa)	starting	2.47	1.23	0.50
	peak	19.51	16.02	19.46
	net increase	17.04	14.79	18.96
	peak/static	9.9	8.1	9.9
VP_m (kPa)	starting	7.15	8.49	8.56
	peak	17.53	16.91	18.27
	net increase	10.38	8.42	9.71
	peak/static	2.8	2.7	2.9
LP_m (kPa)	starting	2.79	3.02	2.91
	peak	20.03	17.49	19.90
	net increase	17.24	14.47	16.99
	peak/static	6.7	5.8	6.7
VP_B (kPa)	starting	9.21	11.04	11.28
	peak	16.39	16.57	18.17
	net increase	7.18	5.53	6.89
	peak/static	2.5	2.5	2.8
LP_B (kPa)	starting	3.54	3.09	3.15
	peak	31.95	26.17	31.54
	net increase	28.41	23.08	28.39
	peak/static	10.6	8.7	10.4

Note: 1. VP = vertical pressure; LP = Lateral pressure.
2. $_T$ = top level; $_M$ = middle level; $_B$ = bottom level.

increase in the average grain moisture from 9.3 to 15.4% (Fig. 5.8). For a grain moisture increase of 6.1%, the vertical force on the wall changed from +2.47 (downward) to -5.98 kN (upward)(Fig. 5.8). This suggests that the upward lifting force caused by grain bulk expansion would have lifted the bin wall up from the base if the wall had not been tied down properly. When both vertical loads reached their peak values, the increase in total grain mass due to moisture gain was 5.6%. This grain mass increase alone should cause a 5.6% increase in both vertical loads (downward) on the floor and on the wall, which were calculated to be 0.36 and 0.14 kN, respectively. By taking these increases into account, the vertical force (upward) on the wall due to bulk expansion was calculated to be 8.59 kN and the increase in vertical force on the floor was also 8.59 kN. In fact, by excluding the effect of grain mass increase on both vertical loads, the curve of vertical force on the wall is a mirror image of that of vertical force on the floor. This was because that the reaction of bulk expansion force on the wall also acted on the floor through the grain bulk. During the first, second, and third wetting cycles, the bulk expansion force were 8.07, 7.30, and 8.59 kN and represented 93.4, 94.9, and 96.0% of vertical force increase on the floor, respectively. Grain mass increase contributed only 4.0 to 6.6% of increases in vertical force on the floor. Similarly, the increase in grain mass affected only 1.6 to 4.1% of variation in the vertical force on the wall. This means that vertical floor and wall loads during wetting were dictated by the grain bulk expansion. Peak vertical forces on the floor were 2.2 to 2.5 times as great as their respective starting values, and 2.5 to 2.7 times as high as the static floor load. The magnitudes of the peak frictional forces (upward) were 1.4 to 2.4 times as great as their

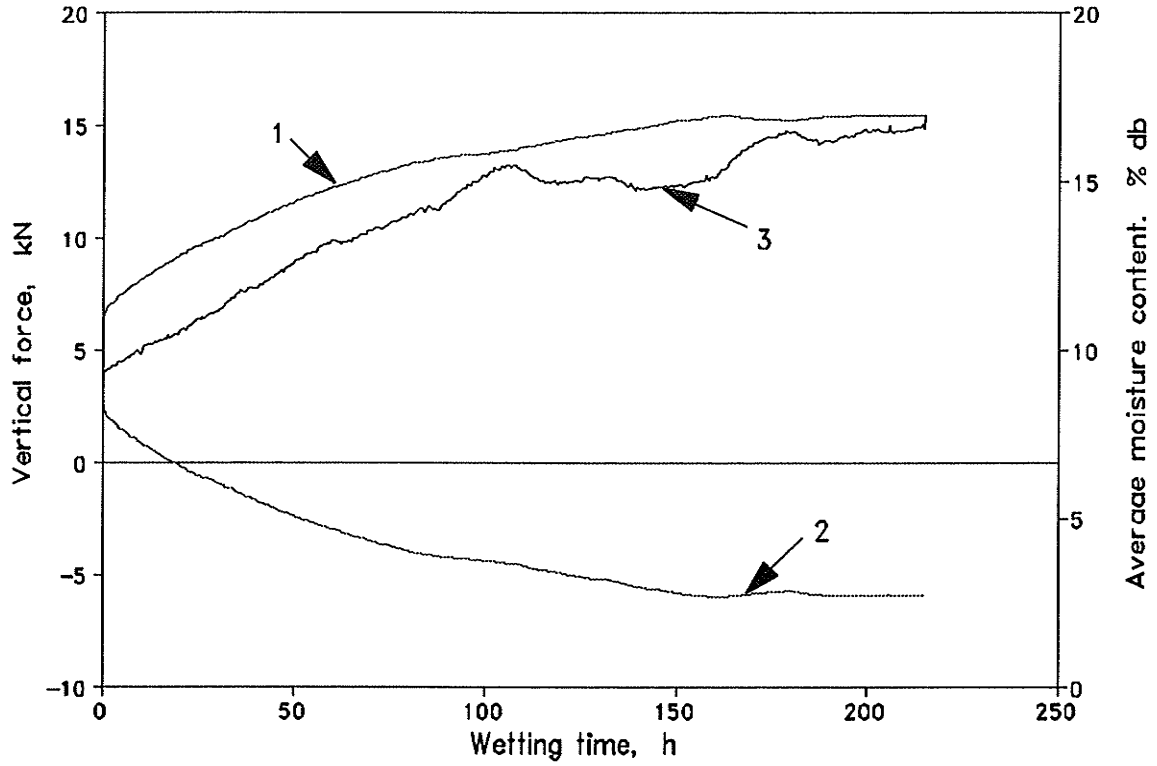

Fig. 5.8 Vertical forces on the floor and wall during the third wetting cycle. 1-vertical force on floor; 2-vertical force on wall; 3-average moisture content of grain.

respective starting values (downward) and peak DSRs ranged between 1.2 and 1.6.

Regression analysis indicated that the vertical force on the wall had good linear relationships with the AMC of the grain if the AMC of the grain increased steadily during wetting. At the beginning of the first wetting cycle, the AMC of the grain dropped slightly (by 0.4%)(Fig. 5.9), probably because of a high grain temperature. The starting temperature averaged from the three measuring levels were 26.0 ^{0}C for the first wetting cycle, which was 2.8 ^{0}C and 4.3 ^{0}C higher than those for the second and third cycles, respectively. The starting grain temperature in the top area was 3 ^{0}C higher than that of the grain in the bottom area. At the beginning of wetting, the grain in the lower section of the bin was cooled down and wetted by the air, but in the upper section the grain lost moisture to the air due to a high grain temperature at which the grain had a low moisture holding capacity, resulting a AMC decrease. As wetting progressed, the grain in the whole bin was cooled down and the AMC increased. The regression equations for vertical force on the wall with AMC were:

VF_w = -101.84 AMC+10.78 (kN) (for the AMC from 8.7 to 12.0%), and

VF_w =-28.56 AMC+21.00 (kN) (for the AMC from 12.0 to 15.8%),

both with R^2 >=0.98. During the third wetting cycle (Fig 5.10), the regression equations were:

VF_w = -188.42 AMC +19.77 (kN) (for the AMC from 9.3 to 10.8%), and

VF_w =-108.25 AMC +11.24 (kN) (for the AMC from 10.8 to 14.2%),

both with R^2 >= 0.99. The AMC fluctuated after it became greater than 15.8 % during the first wetting cycle and 14.2 % during the third, which indicated that the grain

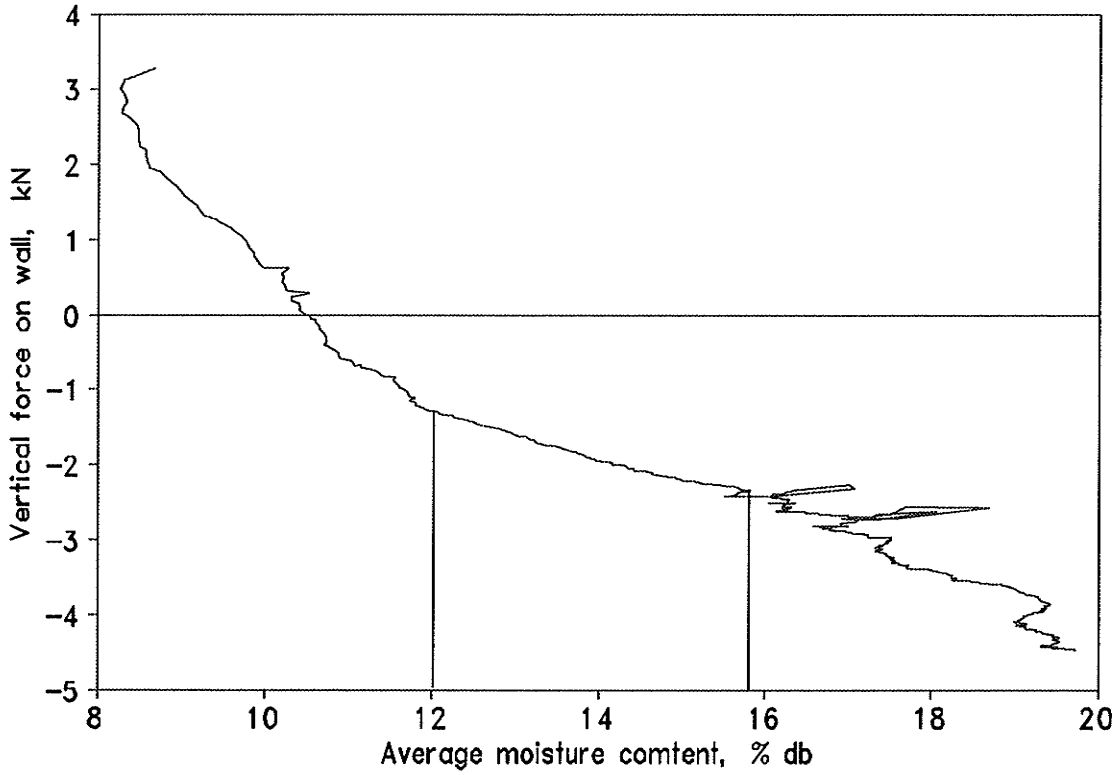

Fig. 5.9 Variations of vertical force on the wall with the average moisture content of the grain during the first wetting cycle.

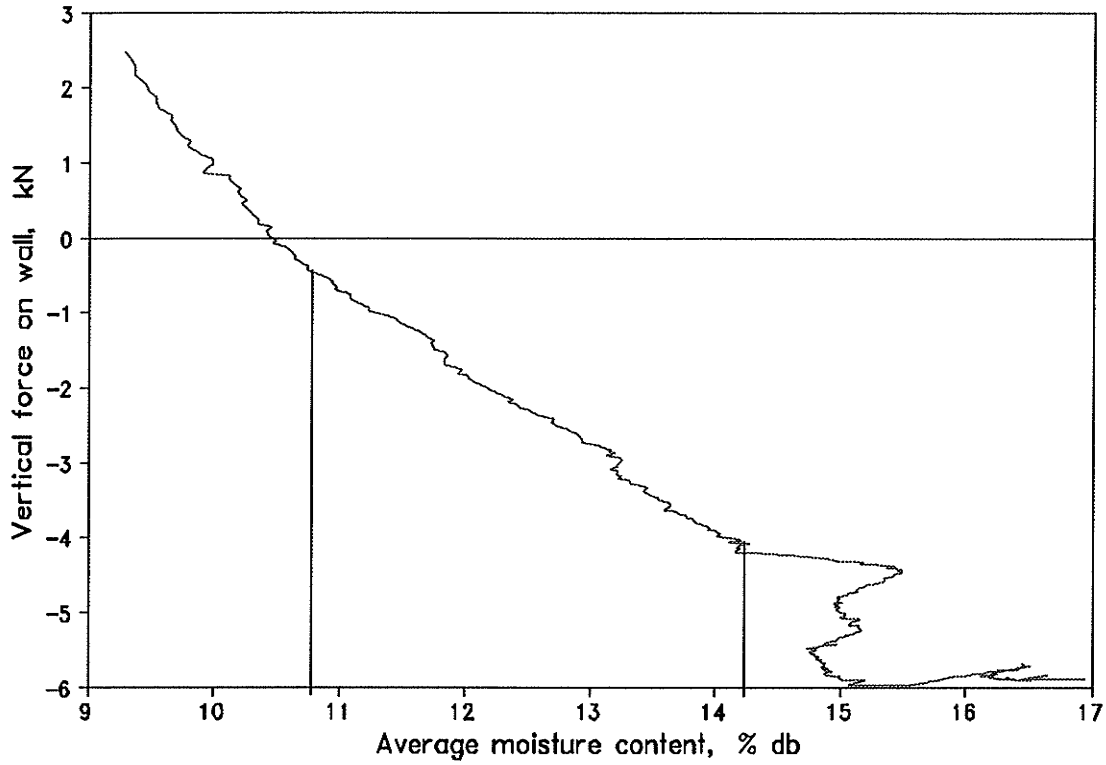

Fig. 5.10 Variations of vertical force on the wall with the average moisture content of the grain during the third wetting cycle.

moisture was equilibrating with the air moisture. For the high moisture ranges, vertical force on the wall increased little when the AMC increased, hysteresis occurred and linear relationship did not exist (Figs. 5.9 and 5.10). This will be discussed later with the lateral pressure as the vertical wall load is dependent on the lateral pressure. The linear relationship were not observed during the second wetting cycle as the AMC fluctuated for the whole process (Fig. 5.11). The regression equation for the vertical wall load with the AMC was as follows (with $R^2 = 0.97$):

$$VF_w = -108.69\ AMC + 12.56\ (kN)\quad \text{(for the AMC from 9.5 to 14.5\%)}.$$

5.4.3 Lateral and Vertical Pressures

Lateral pressure increased at all three levels during all three wetting cycles (Table 5.3). The greatest increase in lateral pressure occurred at the bottom level during each wetting cycle. During the first wetting cycle, lateral pressure at the bottom level increased from 3.54 to 31.95 kPa, or 9.0 fold when the AMC of the grain increased from 8.7 to 19.7%. Compared with the static loads (a lateral pressure of 3.02 kPa and a vertical pressure of 6.56 kPa at the bottom level), this represented an overpressure of 28.93 kPa, or an OPF of 10.6 for an increase of 9.9% in average grain moisture (The grain moisture at the bottom level was estimated to be 24% based on probe sampling at the end of the first wetting cycle). Using a Poison's ratio of 0.4, an initial kernel density of 1383.7 kg/m^3 (Brusewitz 1975), a final kernel density of 1349.7 kg/m^3 (Brusewitz 1975), a tangent bulk modulus (M_i) of 498.8 kPa and an asymptotic value of volumetric strain ($\varepsilon_{v,ult}$) 13.580% (both M_i and $\varepsilon_{v,ult}$ were interpolated from Smith and Lohnes 1983), the prediction equation developed by Zhang et al. (1995) gives an overpressure of 35.61

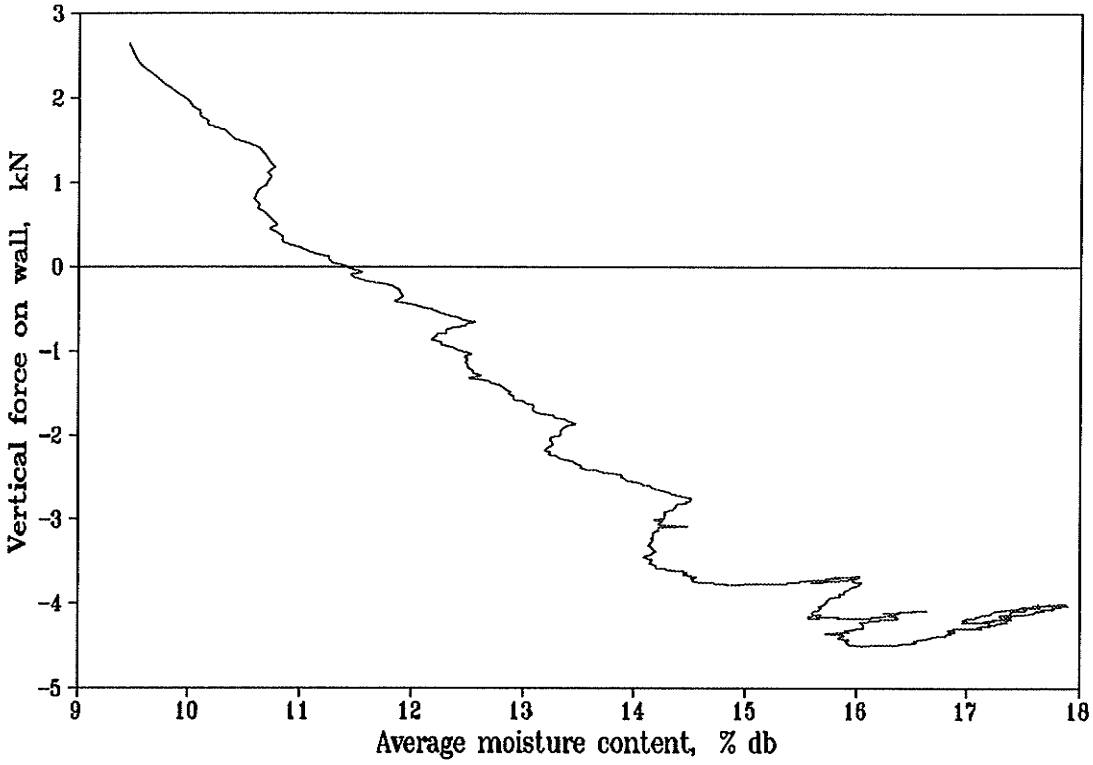

Fig. 5.11 Variations of vertical force on the wall with the average moisture content of the grain during the second wetting cycle.

kPa, or an OPF of 12.8, which is slightly higher than the measured value. During the entire wetting experiment, the peak lateral pressures recorded at the bottom level ranged between 26.17 and 31.95 kPa and were 8.5 to 10.0 times their respective starting values. The OPF ranged between 8.7 and 10.6.

Figs. 5.12, 5.13, and 5.14 illustrate the variations in lateral pressure and average grain moisture during wetting. The profiles of lateral pressure curves are similar for all three cycles. Lateral pressures at all the three measuring levels increased when wetting started. This implies that the air blown through the grain bulk still had ability to add moisture to the grain at the above levels after going through the grain bulk in the bottom section. Increases in lateral pressure were almost the same at the top and middle levels, but much higher at the bottom (Figs 5.12, 5.13, and 5.14). Net increases in lateral pressure at the bottom level were 64.8%, 57.8%, and 59.8% greater than those at the middle level during the first, second, and third wetting cycles, respectively. Large increases in lateral pressure at the bin bottom was observed by Dale and Robinson (1954) for wetted corn. In their experiment, when corn was wetted from an initial moisture of 13.2% to an average of 15.0% wb, increase in lateral pressure at the bottom level was 51.0% greater than that at a higher level, which was only 254 mm above. This is probably attributed to a greater increase in grain moisture at the bottom level, which caused a greater wall friction allowing a higher lateral swelling pressure to be built up. A greater moisture increase was achieved at the bin bottom for three reasons. First, as the air moisture was absorbed by the grain during wetting, the humidified air always had the highest moisture when passing through the bottom section. Second, the grain was

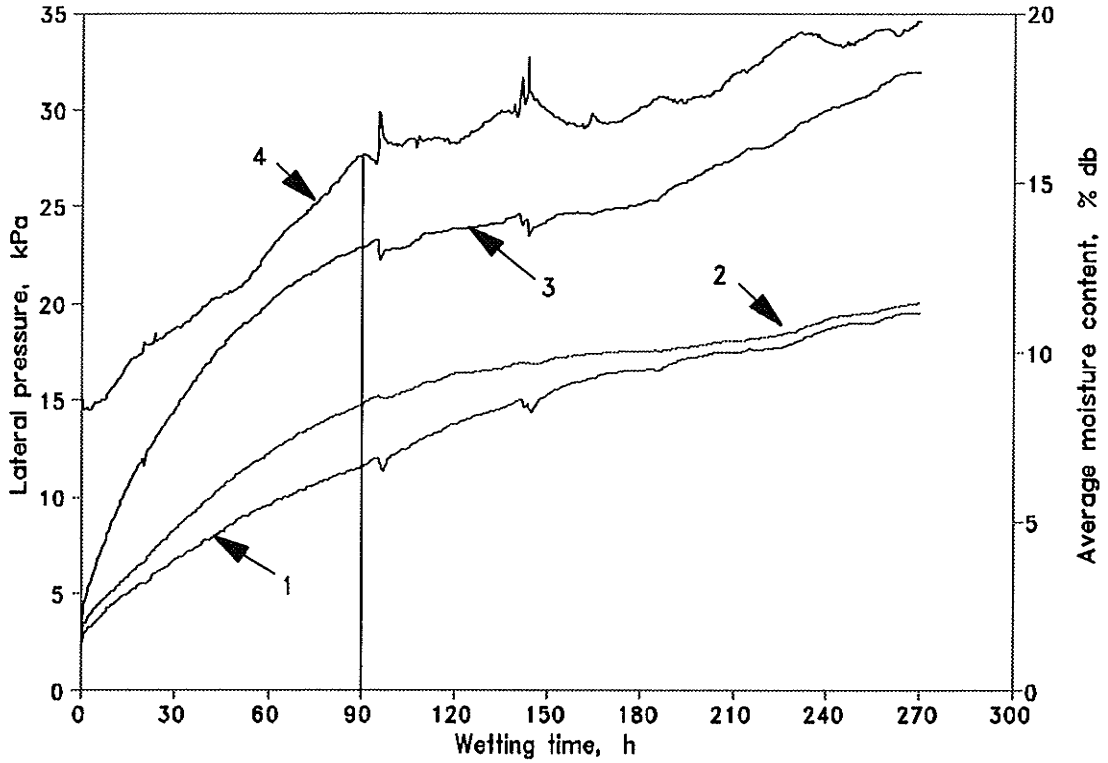

Fig. 5.12 Lateral pressure during the first wetting cycle. 1-lateral pressure at top level; 2-lateral pressure at middle level; 3-lateral pressure at bottom level; 4-average moisture content of grain.

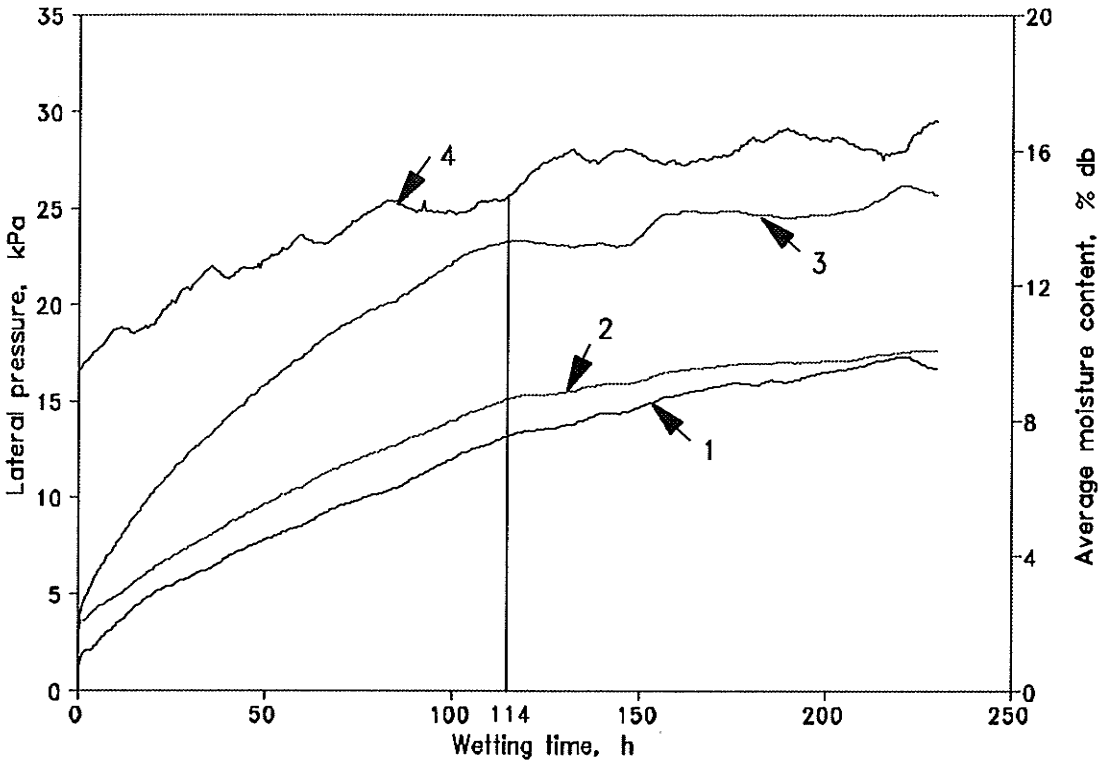

Fig. 5.13 Lateral pressure during the second wetting cycle. 1-lateral pressure at top level; 2-lateral pressure at middle level; 3-lateral pressure at bottom level; 4-average moisture content of grain.

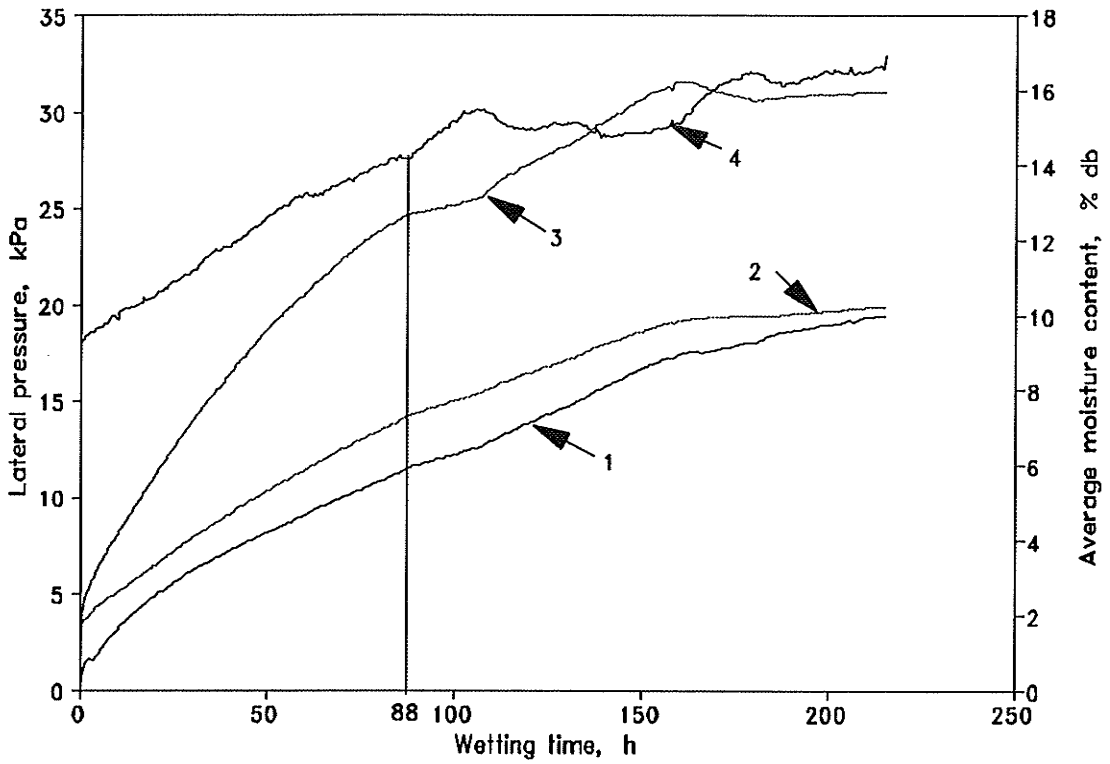

Fig. 5.14 Lateral pressure during the third wetting cycle. 1-lateral pressure at top level; 2-lateral pressure at middle level; 3-lateral pressure at boom level; 4-average moisture content of grain.

drier at the lower section of the bin at the beginning of a wetting cycle when the wetting cycles started after a drying process. Therefore, there was a great drying potential in the lower portion of the bin. In addition, the temperature of grain at the bottom was lowered by the passing air in the early stage, which increased moisture absorbing capacity of the grain. Although the moisture contents of the grain at the measuring levels were not monitored, it is believed that the grain at the bottom level had the greatest moisture increase, which resulted in the highest swelling pressures.

During the first 90 hours in the first wetting cycle, lateral pressure at the bottom level increased from 3.54 to 22.94 kPa, or a net of 19.40 kPa. For only one third of the total wetting time, 68.3% of the total increase in lateral pressure was achieved. This was the direct result of a rapid increase in grain moisture content. During this period, the average moisture content of the grain increased 7.1%, which was 64.5% of the total increase of 11%. For all three wetting cycles, 64.5 to 80.3% of increase in average moisture content and 68.3 to 87.3% of increase in lateral pressure were achieved in the early wetting stages of 88 to 114 hours.

The variations of lateral pressure with the average grain moisture are plotted for the three wetting cycles (Figs. 5.15, 5.16, and 5.17). Changes in lateral pressure at all three measuring levels had the same trend and the variations of lateral pressure followed with those of the vertical wall load (Figs. 5.9, 5.10, and 5.11). During the first and third wetting cycles, lateral pressure at all three levels had good linear relationships with the average grain moisture in the same moisture ranges. When the AMC fluctuated, lateral pressure kept increasing even the AMC decreased. This was probably due to the "inertia"

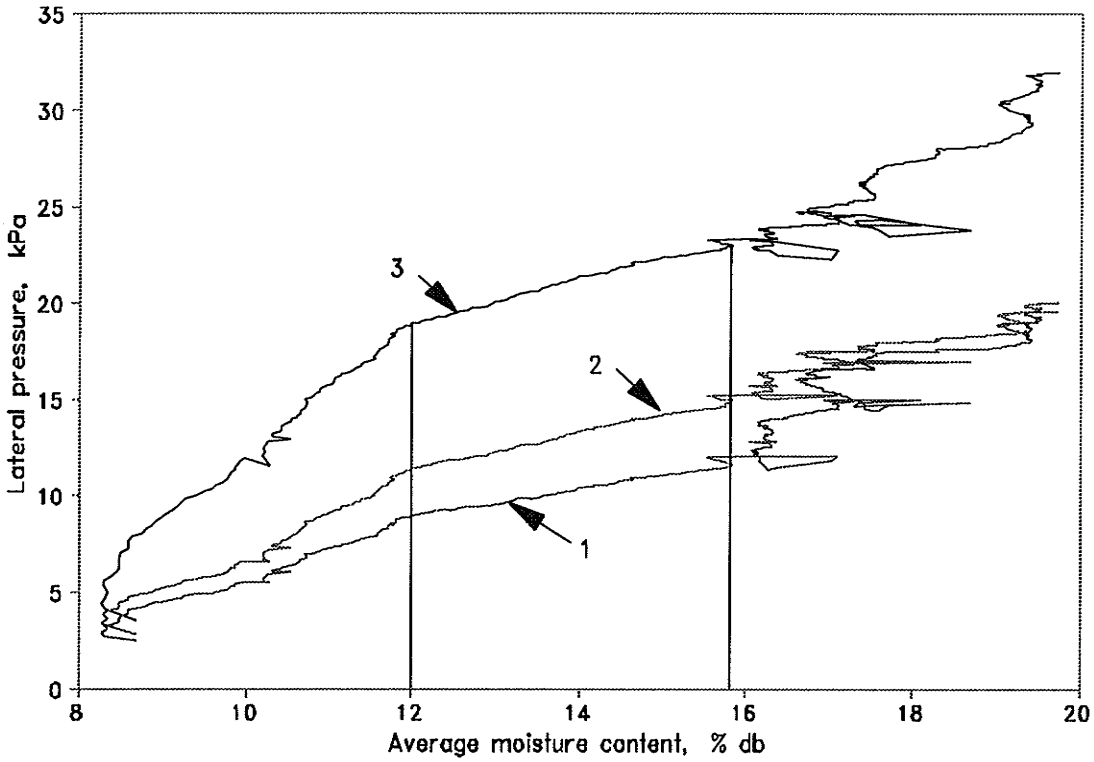

Fig. 5.15 Variations of lateral pressure with the average moisture content of the grain during the first wetting cycle. 1-lateral pressure at top level; 2-lateral pressure at middle level; 3-lateral pressure at bottom level.

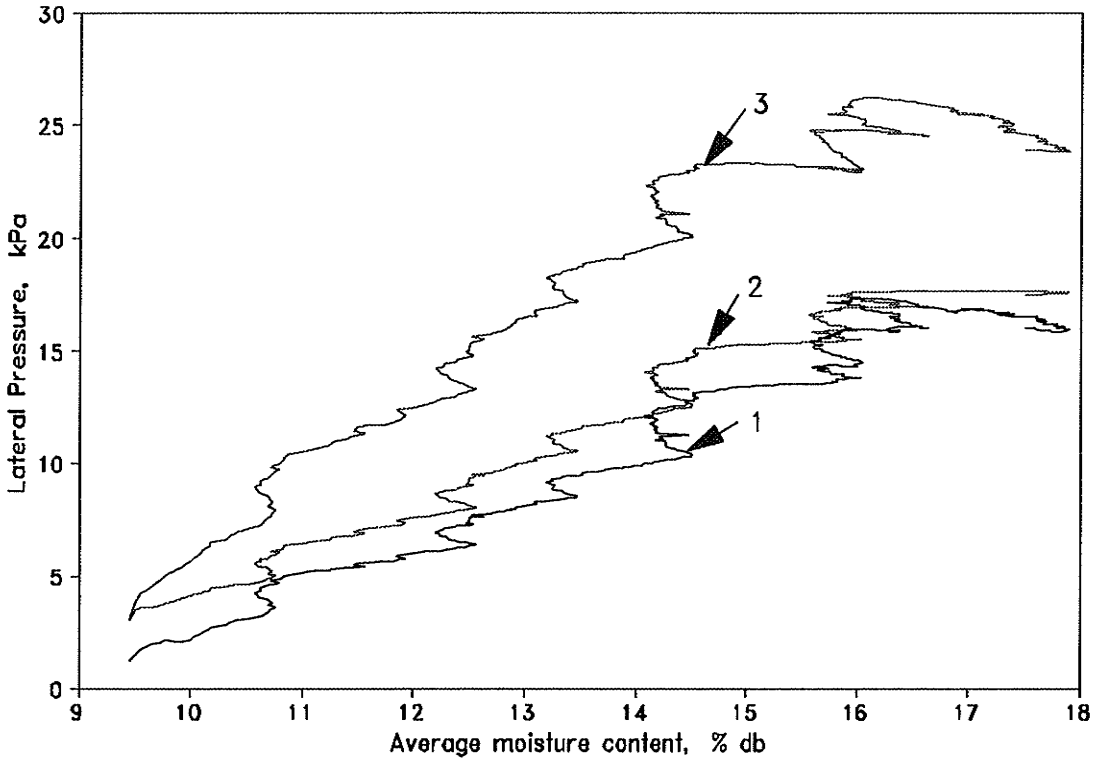

Fig. 5.16 Variations of lateral pressure with the average moisture content of the grain during the second wetting cycle. 1-lateral pressure at top level; 2-lateral pressure at middle level; 3-lateral pressure at bottom level.

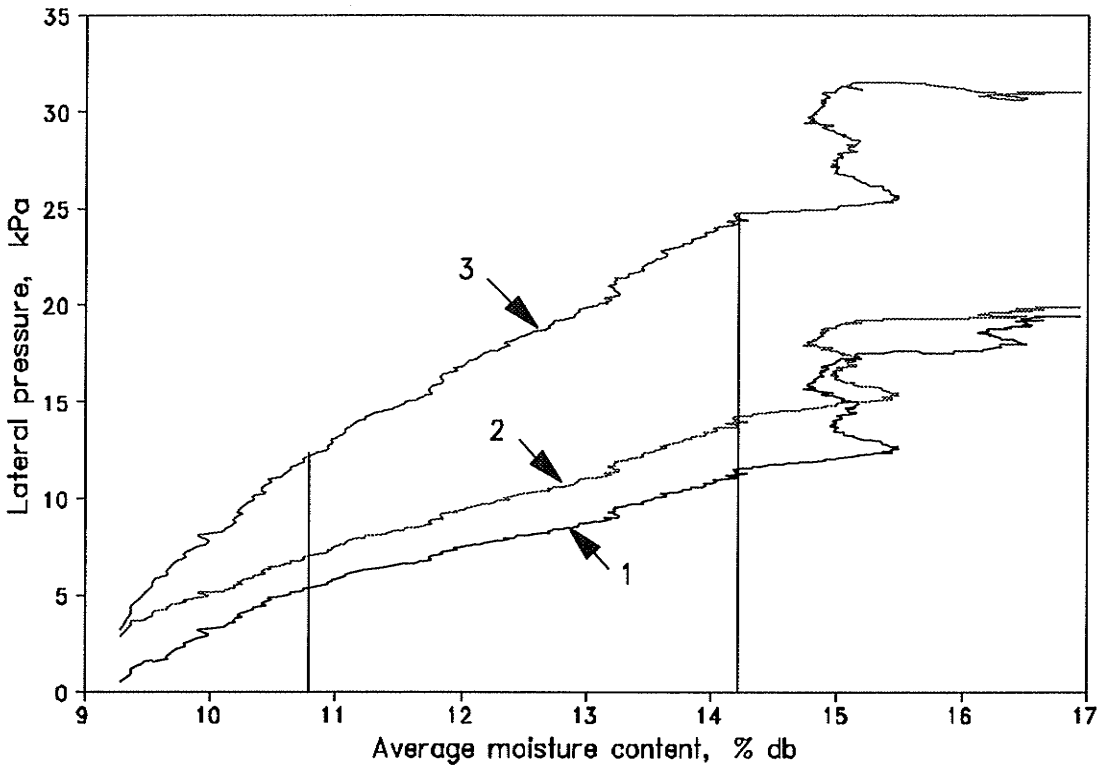

Fig. 5.17 Variations of lateral pressure with the average moisture content of the grain during the third wetting cycle. 1-lateral pressure at top level; 2-lateral pressure at middle level; 3-lateral pressure at bottom level.

of moisture absorption of the grain. As the grain moisture increased, the moisture absorption of the grain slowed down and some moisture from the air accumulated on the surfaces of the grain kernels. Surface moisture was accounted as part of the grain mass used to compute the AMC. Even when the AMC was decreasing, surface moisture continued to be absorbed by the grain, thus swelling continued and lateral pressure kept increasing. This also explains the similar relationship between the wall load and the AMC (Figs. 5.9 and 5.10) as the wall load is dependent on the lateral pressure. The linear relationships between lateral pressure and the AMC was not observed during the second wetting process as the AMC fluctuated for the whole process.

Vertical pressures increased with the grain moisture (Figs. 5.18, 5.19, and 5.20). The greatest increase in vertical pressure occurred at the top level during each of the wetting cycles (Table 5.3). For an increase in the AMC from 8.7 to 19.7% during the first wetting cycle, the vertical pressures increased from 3.03 to 20.23 kPa, 7.15 to 17.53 kPa, and 9.21 to 16.39 kPa at the top, middle, and bottom levels, respectively. In the early wetting stage, vertical pressure at all three levels increased at almost the same speed although grain at a higher level had a less moisture increase. This was because that vertical pressure transmitted upwards through the grain to contribute to the above section. As the moisture equilibrating front moved upwards, vertical pressure increase stopped or slowed down earlier at a lower level, which means that vertical pressure increase lasted a longer period at a higher level. Because of a greater grain-wall friction at a lower level, vertical pressure could hardly transmit downwards even when it was higher at a higher level. This was probably the reason that a higher vertical pressure appeared at a higher

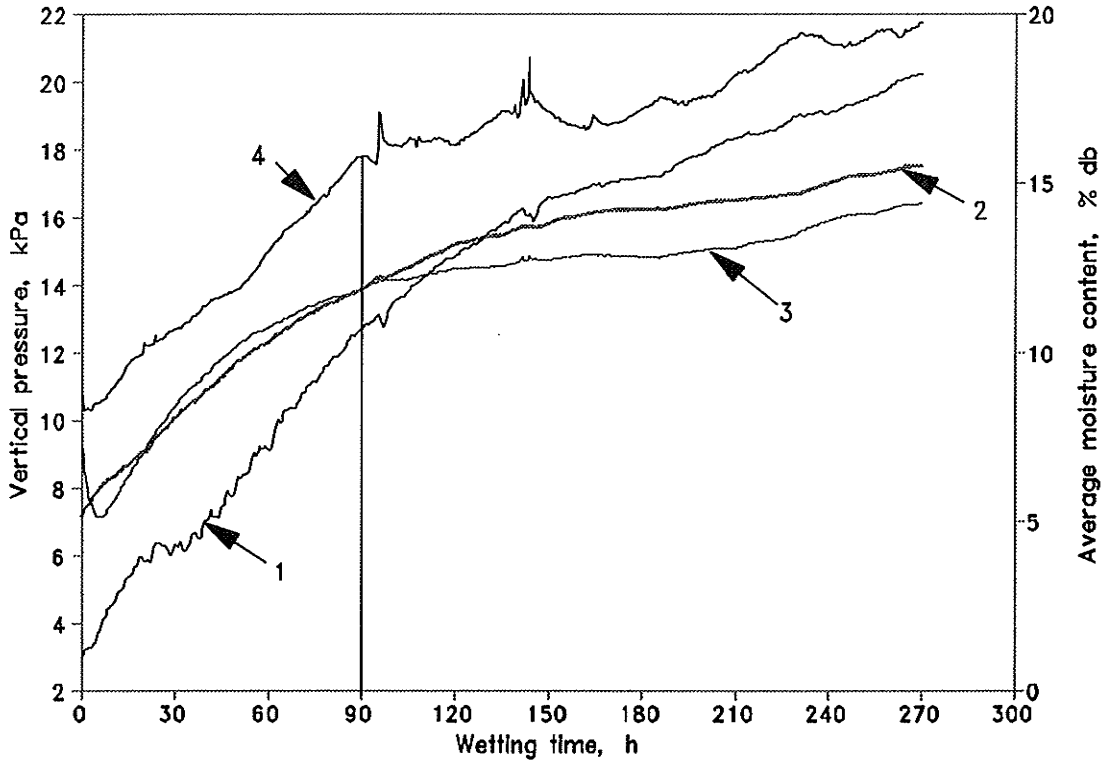

Fig. 5.18 Vertical pressure during the first wetting cycle. 1-vertical pressure at top level; 2-vertical pressure at middle level; 3-vertical pressure at bottom level; 4-average moisture content of grain.

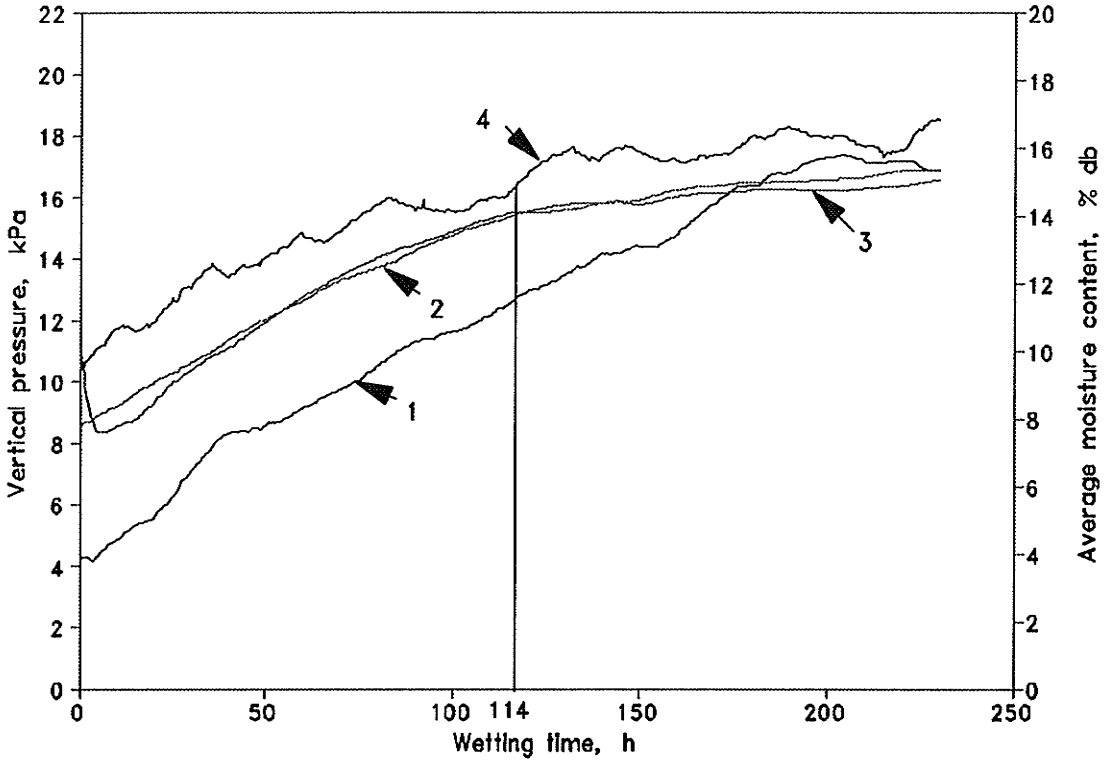

Fig. 5.19 Vertical pressure during the second wetting cycle. 1-vertical pressure at top level; 2-vertical pressure at middle level; 3-vertical pressure at bottom level; 4-average moisture content of grain.

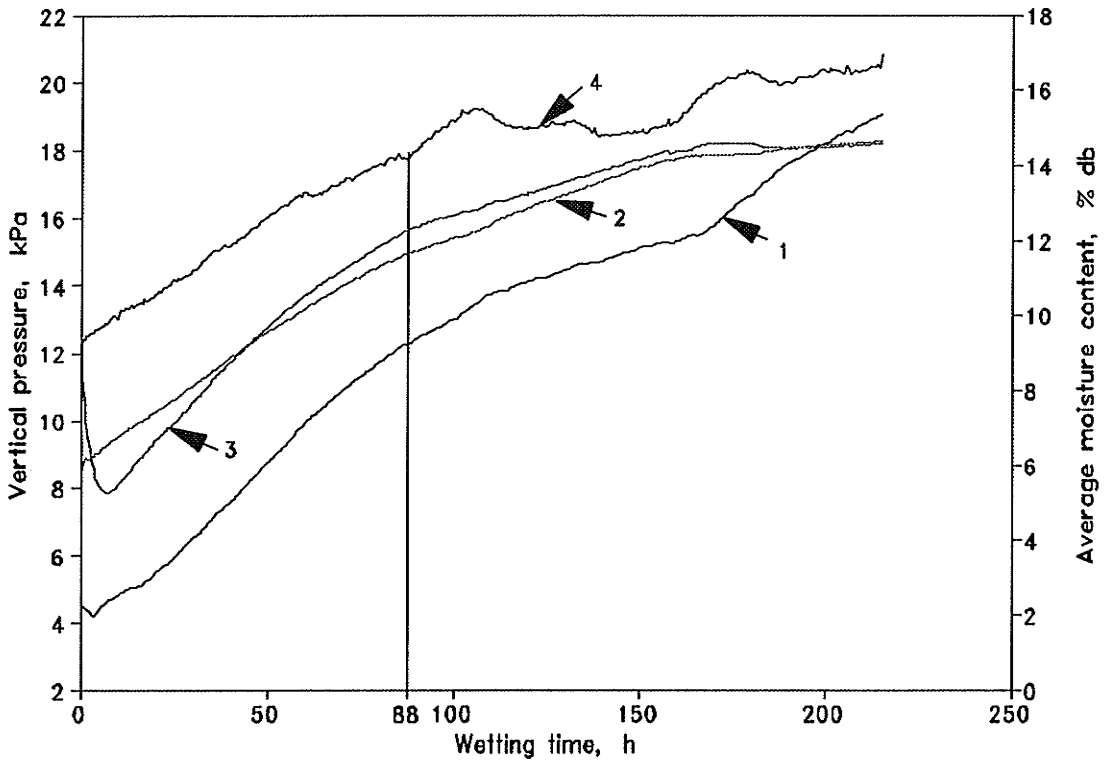

Fig. 5.20 Vertical pressure during the third wetting cycle. 1-vertical pressure at top level; 2-vertical pressure at middle level; 3-vertical pressure at bottom level; 4-average moisture content of grain.

level in the final wetting stage. During the three wetting cycles, peak vertical pressure at the top level ranged between 17.06 and 20.23 kPa, which were 4.1 to 6.7 times as great as their respective starting values.

At the beginning of wetting (within seven hours), vertical pressure at the bottom level dropped slightly (Figs. 5.18, 5.19, and 5.20). This might be attributed to increase in grain-wall friction caused by rapid increases in grain surface moisture and lateral pressure. The grain-wall friction increase reduced the vertical pressure, but in the meantime, swelling pressure in vertical direction was not high enough to compensate the reduction. As wetting progressed, the vertical pressure increased because swelling pressure became dominant. Vertical pressure curves levelled off first at the bottom, then middle, and top levels, which followed the order in which the grain moisture at the three levels equilibrated with the air moisture. During the first wetting cycle, the average vertical pressure calculated from the measured vertical force on the floor (14.28 kN) was 18.06 kPa, which was 10.2% higher than the measured value (16.39 kPa).

Two sudden drops, which were recorded in most of the pressure curves during the first wetting cycle (Figs. 5.9 and 5.18), might imply that there were releases of bulk expansion when local friction was overcome.

Variations of the lateral to vertical pressure ratio (K) are showed in Fig. 5.21. The lateral to vertical pressure ratio increased sharply at all three levels during the initial wetting stage and then approached to a constant value. The pressure ratio fluctuated most at the top level probably due to the movement of the grain at this level, which affected the stability of the measurement. Variations of K were consistent at the bottom and

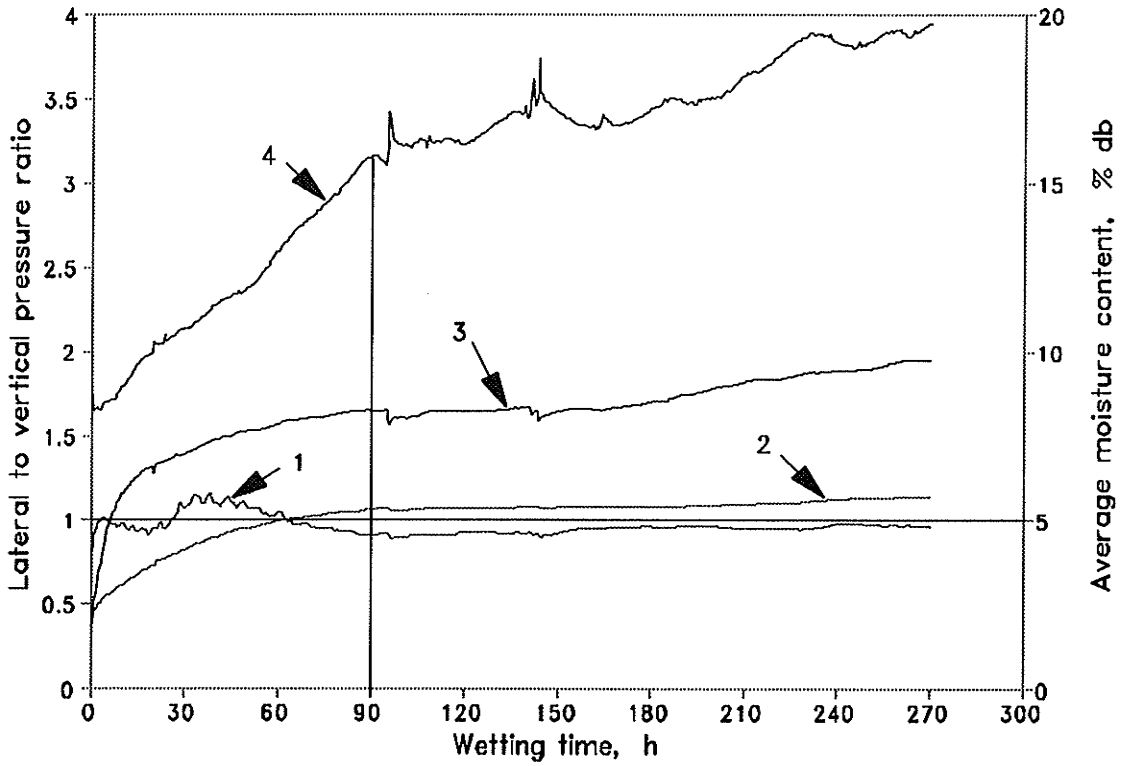

Fig. 5.21 Lateral to vertical pressure ratio (K) during the first wetting cycle. 1-K at top level; 2-K at middle level; 3-K at bottom level; 4-average moisture content of grain.

middle levels. The highest observed K of 1.95 occurred at the bottom level during the first wetting cycle when the average grain moisture changed from 8.7 to 19.7%. During the three wetting cycles, the peak values of K ranged between 1.58 and 1.95 at the bottom level. This indicated that lateral pressure increased much more than the vertical when grain was wetted.

5.5 Bin Loads During Subsequent Drying Cycles

Wetted grain was dried from an average moisture range of 16.5 to 19.5% to a range of 9.2 to 9.4% right after each wetting cycle. There appeared a turning point in the curves of vertical forces on the floor and wall after 24 to 48 h of drying (Fig. 5.22). Before the turning point, the vertical force on the floor dropped quickly, and the upward frictional force on the wall decreased to zero and then reversed its direction. This was attributed to decreases in swelling pressures and grain-wall friction. As drying started after wetting, higher moisture in grain surface area dropped rapidly and grain kernels shrank, which decreased the grain-wall friction and swelling pressures. Both vertical forces on the floor and wall returned to values close to those at static conditions at the turning point and approached to a constant value during further drying even though the grain moisture continued to decrease. This indicated that vertical floor and wall loads due to grain swelling vanished. The turning point appeared at average moisture contents of 18.0, 15.0, and 13.3% during the first, second, and third drying cycles, respectively. The vertical floor load was slightly greater and the vertical frictional force on the wall was slightly lower at the end of a later cycle (Table 5.4).

Variations of vertical and lateral pressures followed the movement of drying

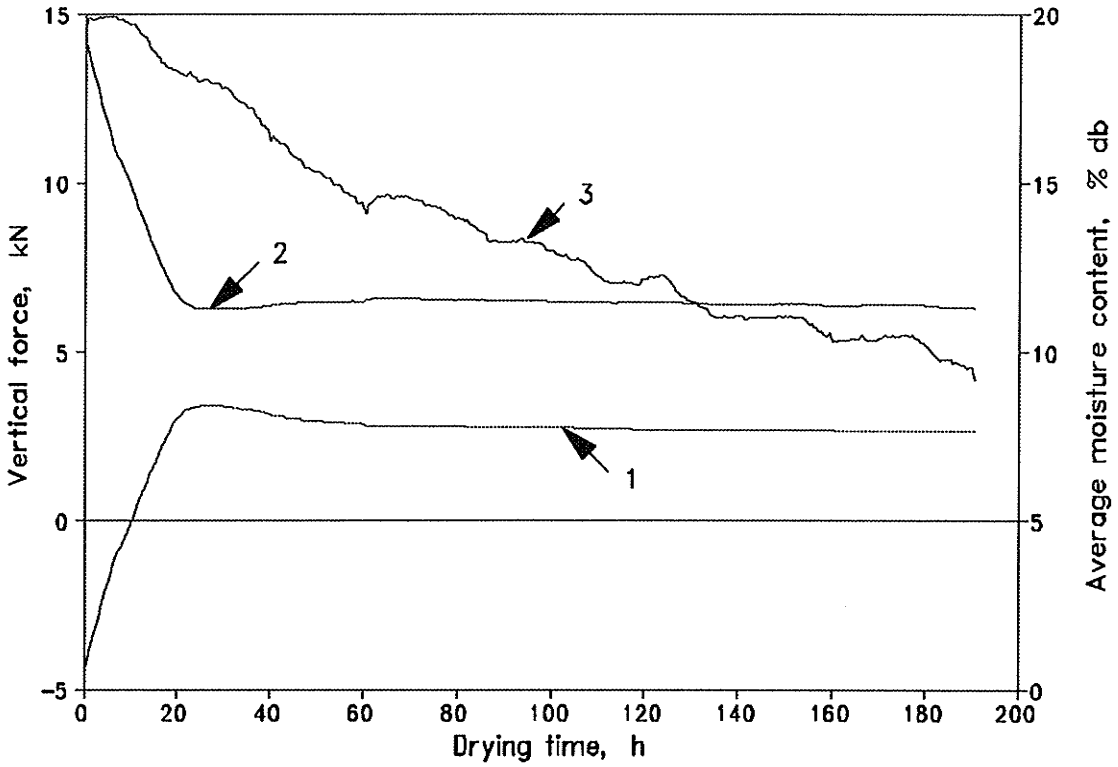

Fig. 5.22 Vertical forces on the floor and wall during the second drying cycle. 1-vertical force on wall; 2-vertical force on floor; 3-average moisture content of grain.

fronts: vertical and lateral pressures remained unchanged until a drying front arrived, decreased rapidly as the drying front was passing through, and tended to stay constant after the drying front had passed (Figs. 5.23, 5.24, and 5.25). A turning point appeared in the pressure curves at the bottom level at the same time as in the vertical force curves (Fig, 5.25), which implied that swelling pressure and grain-wall friction at the bottom dictated vertical wall load during wetting.

Table 5.4 Vertical forces on the floor and wall during drying of wetted grain

	DC 2		DC 3		DC 4	
AMC,% db	19.6	9.2	17.5	9.4	16.5	9.2
VF_f, kN	14.16	6.29	13.62	6.46	15.22	6.60
VF_w, kN	-4.37	2.65	-4.00	2.49	-5.69	2.34

Note: VF_f = vertical force on the floor; VF_w = vertical force on the wall.

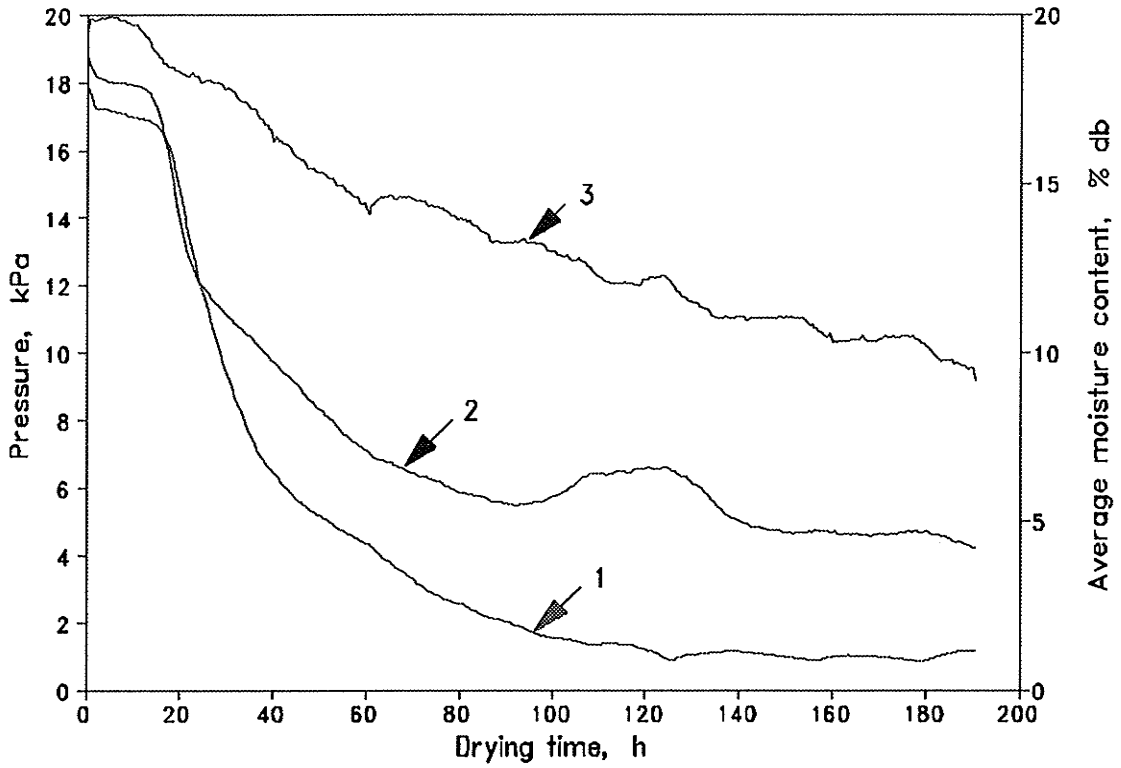

Fig. 5.23 Lateral and vertical pressures at the top level during the second drying cycle. 1-lateral pressure; 2-vertical pressure; 3-average grain moisture of grain.

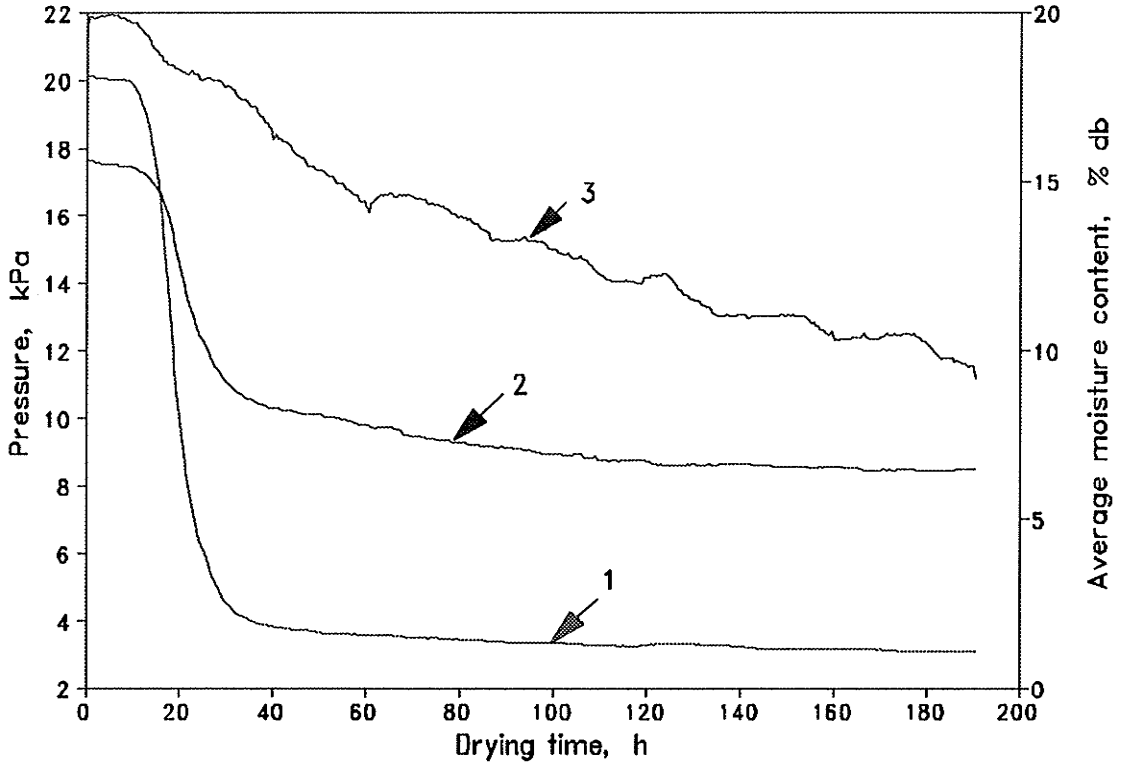

Fig. 5.24 Lateral and vertical pressures at the middle level during the second drying cycle. 1-lateral pressure; 2-vertical pressure; 3-average grain moisture of grain.

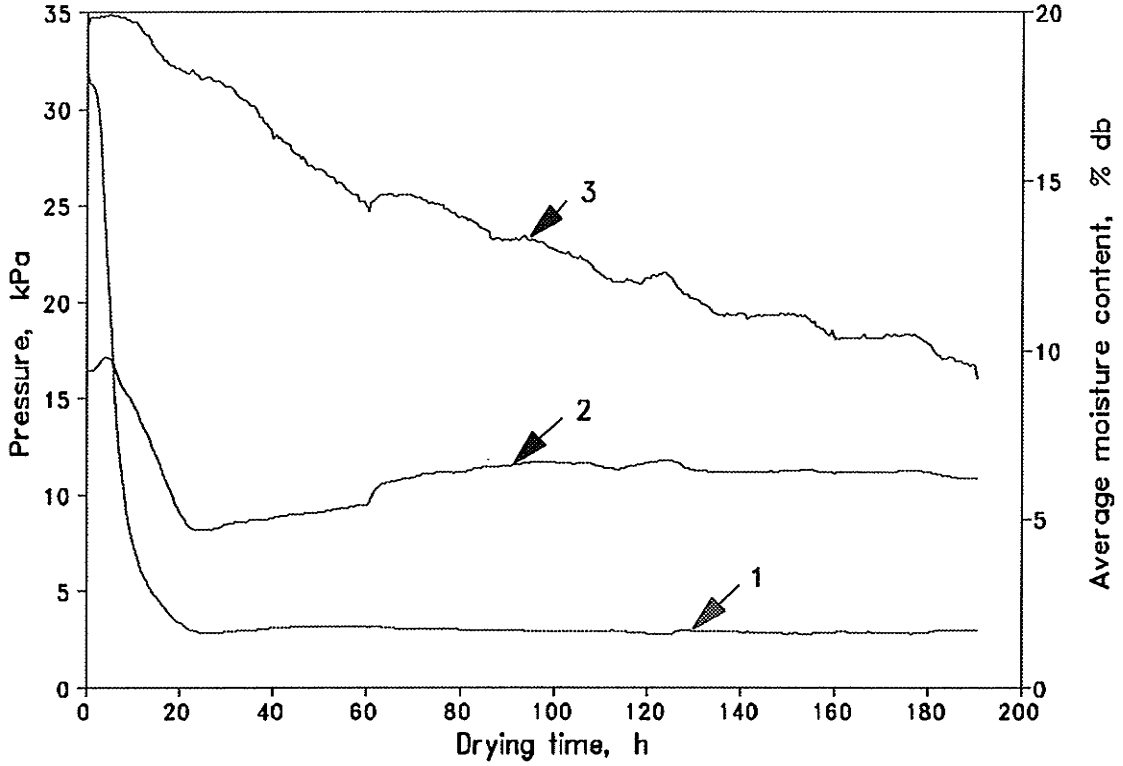

Fig. 5.25 Lateral and vertical pressure at the bottom level during the second drying cycle. 1-lateral pressure; 2-vertical pressure; 3-average moisture content of grain.

Chapter 6

SUMMARY AND CONCLUSIONS

An experiment was conducted to study loads in grain bins during the drying of stored grain with near-ambient air. A corrugated steel model bin, 0.96 m in diameter and 1.57 m high, was used in the experiment. Vertical forces on the floor and wall were measured separately with force transducers. Lateral and vertical pressures at three depths in the grain mass were recorded using diaphragm pressure sensors. The pressure sensors were installed in pair at each depth with one measuring vertical pressure and the other measuring the lateral. All three pairs of sensors were placed 100 mm radially from the outer extreme of the bin wall and 384 mm apart vertically starting 140 mm from the bin floor. Freshly-harvested red hard spring wheat was first dried from an initial moisture of 14.1% db to an average of 11.0% by blowing near-ambient air through the grain bed and then three wetting-drying cycles were performed between average moisture contents of 8.7 and 19.7%. Wetting processes were conducted by blowing near-saturated air through the grain bulk. The results of this study showed that:

1. The lateral and vertical pressures measured by diaphragm pressure sensors under static conditions were in agreement with those predicted by Janssen's equation. The average ratio of lateral to vertical pressure calculated from the measured pressures was 0.47 at a moisture content of 14.1% db.
2. When the grain was dried from an initial moisture of 14.1% db to an average of 11.0%, vertical frictional force on the wall decreased from 3.72 to 3.37 kPa, or 9.4%, and vertical force on the floor increased from 5.63 to 5.74 kPa, or 2.0%.

Vertical pressure in the grain mass increased from 6.56 to 10.11 kPa at the bottom level, 6.37 to 7.87 kPa at the middle level and lateral pressures remained almost constant at these two levels. Both pressures fluctuated at top level.

3. When grain was wetted in an average moisture range from 8.7 to 19.7%, the maximum vertical force on the floor reached 15.43 kN, or 2.7 times as great as its static value. During wetting, vertical resultant force on the wall reversed its direction from downward to upward. The maximum wall load was -5.98 kN (upward), or 1.6 times as great as the static wall load (downward). Expansion force of wetted grain was responsible for 93.3 to 96.0% of increase in vertical force on the floor. Only 4.0 to 6.7% of increase in vertical floor load was caused by grain mass increase. Increase in grain mass contributed only 1.6 to 4.1% to changes in force on the wall.

4. During wetting, the greatest lateral pressure occurred at the bottom level and reached up to 31.95 kPa, or 10.6 times as great as its static value. The greatest vertical pressure was observed at the top level and was as high as 20.23 kPa, or 5.0 times the static value. The greatest ratio of lateral to vertical pressure was as high as 1.95, which occurred at the bottom level.

From this study, the following conclusions were drawn:

1. The ratio of lateral to vertical pressure measured by diaphragm pressure sensors under static conditions was higher than that calculated by Rankine's equation, which is recommended by most design standards and codes.

2. Wetting of grain greatly increased vertical floor load and reversed the direction

of vertical frictional force on the wall from downward to upward. Both vertical floor and wall loads were dictated by expansion force of wetted grain during wetting, not the grain weight changes.

3. Both vertical and lateral pressures increased as grain was wetted. Lateral pressure at the bottom section was much higher than that at the upper section of the bin. The greatest overpressure factor observed at the bottom level was 10.6. At the bottom level, lateral pressure increased much more than did vertical pressure. The maximum lateral to vertical pressure ratio K was 1.95.
4. Drying of wetted grain brought bin loads back to the levels that were close to those existed at the beginning of wetting processes.
5. Variations of both lateral and vertical pressures followed movements of the drying front: both pressures remained unchanged until the drying front arrived, decreased quickly as the drying front was passing through, and changed very little once the drying front had passed through.

The following recommendations were forwarded for further studies:

1. In-bin grain moisture contents should be monitored at measuring levels as local grain moisture dictates local swelling pressures;
2. Other types of grains should be tested because their hygroscopic natures and surface features are different;
3. Different bin walls should be tested as grain-wall friction strength may affect both swelling pressures and vertical loads;
4. Full-size bin tests should be conducted because model tests may not well represent

conditions in full-size bins.

REFERENCES

Airy, W. 1897. The pressure of grain. Proceedings of Institution of Civil Engineering, London. 131:347-358.

ASAE. 1990. Moisture content measurement-unground grain and seeds. ASAE standards, S532.2. ASAE, St. Joseph MI. 387.

Atewologun, A.O. and G.L. Riskowski. 1991. Experimental determination of Janssen's stress ratio by four methods for soybeans under static conditions. Transactions of the ASAE. 34(5): 2193-2198.

Bickert, W.G. and F.W. Buelow. 1966 Kinetic friction of grains on surfaces. Transactions of the ASAE. 9(1):129-131

Blight, G.E. 1986. Swelling pressure of wetted grain. Bulk Solids Handling. 6(6):1135-1140.

Britton, M.G. and N.J. Klassen. 1987. Wheat friction on steel. ASAE Paper No.87-4527.

Britton, M.G., Q. Zhang, and K. McClluagh. 1993. Moisture induced vertical loads in model grain bin. ASAE Paper No.93-4503. St. Joseph, MI:ASAE.

Browne, D.A. 1962. Variation of the bulk density of cereals with moisture content. J. Agric. Eng. Res. 7(4):288-290.

Brubaker, J.E. and J. Pos. 1965. Determining the static coefficients of fiction of grains on structural surfaces. Transactions of the ASAE. 8(1):53-55.

Brusewitz, G.H. 1975. Density of rewetted high moisture grains. Transactions of the ASAE. 18(5):935-938.

Bushuk, W. and Hlynka. I. 1960. Weight and volume changes in wheat during sorption and desorption of moisture. Cereal Chemistry. 37:390-398.

Caughey, R.A., C.W. Tools, and A.C. Scheer. 1951. Lateral and vertical pressure of granular material in deep bins. Bulletin 173, Engineering Experiment Station, Iowa State College, Ames.

Chung, D. S. and H. H. Concerse. 1971. Effect of moisture content on some physical properties of grains. Transactions of the ASAE. 14(4):612-620.

Clower, R.E., I.J. Ross, and G.M. White. 1973. Properties of compressible granular materials as related to forces in bulk storage structures. Transactions of the ASAE.

16(3):478-481.

Collin, H. and I.A. Peschl. 1963. Determining pressures in cylindrical storage structures. Transactions of the ASAE. 6(2):98-101,103.

Dale, A.C. and R.N. Robinson. 1954. Pressure in deep grain storage structures. Agric. Eng. 35(8):570-573

Dougan, K.D. 1992. Stochastic modelling of in-bin drying of wheat with near-ambient air. M.Sc. Thesis. Dept. of Agric. Eng., The University of Manitoba, Winnipeg, MB. 108p.

Galili, N. and S.A. Thompson. 1989. Accurate strain measurement in granular media. ASAE Paper No.89-4540. St. Joseph, MI:ASAE.

Gustafson, R.J. and G.E. Hall. 1972. Density and porosity changes of shelled corn during drying. Transactions of the ASAE. 15(3):523-525.

Hall, G.E. 1963. Unpublished progress reports. Ohio Agric. Exp, Sta., Wooster, Ohio, Project H-218-1 and NC-48.

Hao, D. 1992. Effects of moisture content of stored grain and vibration on dynamic loads during discharge in a corrugated steel model bin. M.Sc. Thesis. Dept. of Agric. Eng., The University of Manitoba, Winnipeg, MB. 95p.

Isaacson, J.D. and J.S. Boyd. 1965. Mathematical analysis of lateral pressures in flat-bottomed deep grain bins. Transactions of the ASAE. 8:358-360,364.

Jaky, D. 1948. Pressures in silos. Pages 1:103-108 in Proceedings of the Second International Conference of Soil Mechanics and Foundations.

Jamieson, J.A. 1903. Grain pressures in deep bins. Transactions, Canadian Society of Civil Engineers. 17:554-654.

Janssen, H.A. 1895. Versuche uber getreidedruck in silozellen. VDI Zeitschrift 39:1045-1049.

Jones, C.R. and J.D. Campbell. 1953. Micro-determination of endosperm density as a means of mapping moisture distribution in wheat grains. Cereal Chemistry. 30(3):177-189.

Ketchum, M.S. 1919. The design of walls, bins and grain elevators. McGraw-Hill Book Company, Inc. New York. 556p.

Measurements Group. 1989. Catalog 500 Part A-Strain gagelistings. Raleigh, NC: Measurements Group, Inc.

Miles, S.R. 1937. The relation between the moisture content and test weight of corn. J. Ame. Soc. Agr. 29:412-418.

Miller, R. 1984. Risk of collapse can be minimized. World Grain. January:28-30.

Mohsenin, N.N. 1986. Physical Properties of Plant and Animal Materials. 2nd edition, Gordon and Breach Science Publishers, New York, NY. USA. 102-103.

Moore, D.W., G.M. White, and I.J. Ross. 1984. Friction of wheat on corrugated metal surfaces. Transactions of the ASAE. 27(6):1842-1847.

Moysey, E.B. 1979. Active and passive pressures in deep grain bins. Transactions of the ASAE. 22(6):1409-1413.

Moysey, E.B. 1984. The effects of grain spreaders on grain friction and bin wall pressures. J. Agric. Eng. Res. 30:149-156.

Muir, W.E. and R.N. Sinha. 1988. Physical properties of cereal and oilseed cultivars grown in western Canada. Can. Agric. Eng. 30:51-55.

Muir, W.E., R.N. Sinha, Q. Zhang and D. Tuma. 1991. Near-ambient drying of canola. Transactions of the ASAE. 34(5):2079-2084.

National Research Council of Canada. 1977. Canadian Farm Building Code. NRCC No. 15564. Associate Committee on the National Building Code. NRCC. Ottawa, ON.

National Research Council of Canada. 1983. Canadian Farm Building Code. NRCC No. 21312. Associate Committee on the National Building Code. NRCC. Ottawa, ON.

Otten, L., A.G. Meiering, R. Brown and T. Daynard. 1977. Ventilation and low temperature drying of corn. Paper No. 77-107. Can. Soc. Agric. Eng., Ottawa, ON.

Paettie, K.R. and R.W. Sparrow. 1954. The fundamental action of earth pressure cells. Journal of the mechanics and physics of solids. 2:141-155.

Pieper, K. 1969. Investigation of silo loads in measuring models. J. Eng. Ind.,Transactions of the ASME. 91:365-372.

Pokrant, D.G. 1987. The effect of flow rate and eccentric discharge on vertical loads in a model grain bin. M.Sc. Thesis, Dept. of Agric. Eng. The University of

Manitoba, Winnipeg, MB.179p.

Reimbert, M. and A. Reimbert. 1976. Silos: Theory and Practice. Trans Tech Publications. Clausthal-Zellerfeld, Germany. 280p.

Reimbert, M. and A. Reimbert. 1980. Pressures and overpressures in vertical and horizontal silos. In Proc. of the Int. Conf. on Design of silos for strength and flow. 1-6 Powder Advisory Centre, Lodon, England.

Sanderson, D.B. 1986. Evaluation of stored-grain ecosystems ventilated with near-abient air. M.Sc. Thesis. Dept. of Agric. Eng., The University of Manitoba, Winnipeg, MB. 191p.

Sanderson, D.B., W.E. Muir, and R.N. Sinha. 1988. Moisture contents within bulks of wheat ventilated with near-ambient air: experimental results. J. Agric. Eng. Res. 40(1):45-55.

Sinha, R.N., W.E. Muir, D.B. Sanderson and D. Tuma. 1991. Ventilation of bin-stored moist wheat for quality preservation. Can. Agric. Eng. 33(1):55-65.

Smith, D.L. and R.A. Lohnes. 1983. Bulk strength and stress-strain behaviour of four agricultural grains. J. Powder & Bulk Solids Technology. 7(4):1-7.

Smith, A.B.B. and S.H. Simmonds. 1983. Lateral coal pressures in a mass floor silo. Structural Engineering Report No. 113. Dept. of Civil Eng., The University of Alberta, Edmonton, AB.

Snyder, L.H., W.L. Roller and G.E. Hall. 1967. Coefficients of kinetic friction of wheat on various metal surfaces. Transactions of the ASAE. 10(3):411-413,419.

Thompson, S.A. and I.J. Ross. 1983. Compressibility and frictional coefficients of wheat. Transactions of the ASAE. 26(4):1171-1176.

Thompson, S.A., R.A. Bucklin, C.D. Batich, and I.J. Ross. 1988. Variation in the apparent coefficient of friction of wheat on galvanized steel. Transactions of the ASAE. 31(5):1518-1524.

Thompson, S.A. and R.A. Williams. 1990. Lateral pressures in a full-sized corrugated grain bin. ASAE Paper No.90-4541. St. Joseph, MI:ASAE.

Timoshenko, S. and S.Woinowsky-Krieger. 1959. Theory of plates and shells. NewYork: McGraw-Hill Book Co., Inc.

Trahair, N.S. 1985. Structural design criteria for steel bins and silos. International Journal

of Bulk Solids Storage in Silos. 1(2):11-20

Williams, J.C., D. Al-Salman and A.H. Birks. 1987. Measurement of static stresses on the wall of a cylindrical container for particulate solids. Powder Technology 50:163-175.

Williams, R.A., S.A. Thompson and N. Galili. 1989. Vertical pressures in full size and model corrugated bins. ASAE Paper No.89-4537. St. Joseph, MI: ASAE.

White, G.M., L.A. Schaper, I.J. Ross. and G.W. Isaacs. 1962. Performance characteristics of enclosed screw conveyors handling shelled corn and soybeans. Purdue University AES Res. Bulletin No. 740, Table 5, March.

Zhang, Q. and M.G. Britton. 1994. Hygroscopic loads in grain storage bins. ASAE Paper No.94-4034. St. Joseph, MI:ASAE.

Zhang, Q., M.G. Britton, and R.J. Kieper. 1994. Interactions between wheat and a corrugated steel surface. Transactions of the ASAE. 37(3):951-956.

Zhang, Q., M.G. Britton, and S. Xu. 1995. Moisture induced loads in bulk solids storage structures.

Zhang, Q., V.M. Pure, and H.B. Manbeck. 1991. An empirical model for friction force versus relative displacement between maize, rice and soybeans on galvanized steel. J. Agric. Eng. Res. 49(1):59-71.

Zhou, L. 1989a. Unpublished data on a barley drying experiment. Dept. of Agric. Eng., The University of Manitoba, Winnipeg, MB. 64p.

Zhou, L. 1989b. Unpublished data on a barley rewetting experiment. Dept. of Agric. Eng., The University of Manitoba, Winnipeg, MB. 63p.

Watson, R.B. 1986. Influence of grid geometry on the output of strain-gage-based diaphragm pressure transducers. Raleigh, NC:Measurements Group, Inc.

APPENDIX A. CALIBRATION RESULTS FOR FORCE TRANSDUCERS AND PRESSURE SENSORS

Table A.1 Calibration results for force transducers*

Transducer No.	Coefficient (με/N)	ST. DEV.#	R^2
1	0.6724	0.8362	0.99996
2	0.6653	0.9198	0.99995
3	0.6736	2.7065	0.99956
4	0.2481	0.1546	0.99997
5	0.2505	0.1493	0.99997
6	0.2515	0.1747	0.99996

* All results were achieved from means of three replications of calibration
# ST. DEV. = standard deviation
Calibration equation: S = Coefficient * F_a, where S = Strain (με), F_a = Applied forces (N).

Table A.2 Calibration results for pressure sensors*

Sensor No.	Coefficient (με/kPa)	ST. DEV.#	R^2
1	15.6806	0.1438	0.99657
2	22.6665	0.2062	0.99917
3	20.0228	0.2528	0.99841
4	21.3378	0.1671	0.99939
5	16.0504	0.0532	0.99957
6	17.2198	0.1393	0.99935

* All results were achieved from means of three replications of calibration
# ST. DEV. = standard deviation
Calibration equation: S = Coefficient * P_a, where: S = Strain (με), P_a = applied pressure (kPa).

APPENDIX B. DESIGN OF PRESSURE SENSORS

When a diaphragm pressure sensor is designed to measure stresses in agricultural granular materials, the following factors should be considered:

1. The stiffness of the diaphragm relative to that of the grain mass

Arching effects would result in the internal redistribution of an applied load in a mass of granular material contacting a body of different stiffness. As agricultural grain does not have a linear stress-strain curve, it is impractical to match its stiffness to that of a metal diaphragm with well-defined elastic properties. A practice alternative is to make the sensor much stiffer than the grain. It is recommended that the stiffness ratio of transducer to grain mass be ten or higher (Peatttie and Sparrow 1954).

2. The thickness to diameter ratio of the diaphragm

The thickness to diameter ratio influences the magnitude of stress redistribution in measurements of soil pressures (Peattie and Sparrow 1954). It is suggested that the thickness to diameter ratio of the diaphragm should be 0.1 or less (Timoshenko and Woinowsky-Krieger 1959). To ensure a linear output within 0.3% from a circular diaphragm, The recommended maximum deflection is 25 % of the thickness of the plate (Measurements Group, 1982). For the diaphragm sensors used in this study (Fig. 4.3), the deflection at the centre was calculated to be 0.15 mm at the design pressure of 32 kPa. The design pressure was the maximum lateral pressure which may occur during wetting and was calculated by multiplying the maximum static lateral pressure calculated at the bottom of the bin used for this study by ten, which is the greatest overpressure factor found during wetting by Dale and Robinson (1954). The calculated deflection of

0.15 mm was slightly lower than the recommended maximum deflection, 25 % of the thickness of the diaphragm, which is 0.16 mm.

3. The pressure-sensing area

The pressure-sensing area should be smaller than the total contact area to reduce stress concentration at the diaphragm edges, which may cause uneven stress distribution across the sensing area (Peatttie and Sparrow 1954). For maximum accuracy and minimum hysteresis, it is a common practice to design a pressure sensor so the sensing area is a part of the integral transducer body (Measurements Group 1982). The pressure sensors for this study were designed as an aluminum disk with its central part machined into a diaphragm. The schema of the pressure sensor is in Fig. 4.3.

4. The configuration of the strain gage grid on the diaphragm

For each diaphragm sensor used in this study, four linear grids were employed and all of them are axially aligned. Although this grid configuration is slightly less sensitive than the arrangement with two inner grids transversely aligned and two outer grids axially aligned, which produces the highest transducer output, it cost less (Watson 1986).

APPENDIX C. TEMPERATURE AND BIN LOAD GRAPHS

The graphs on the following pages are plots of grain temperature with time and bin loads with time during drying and wetting, which do not appear in the text of this thesis.

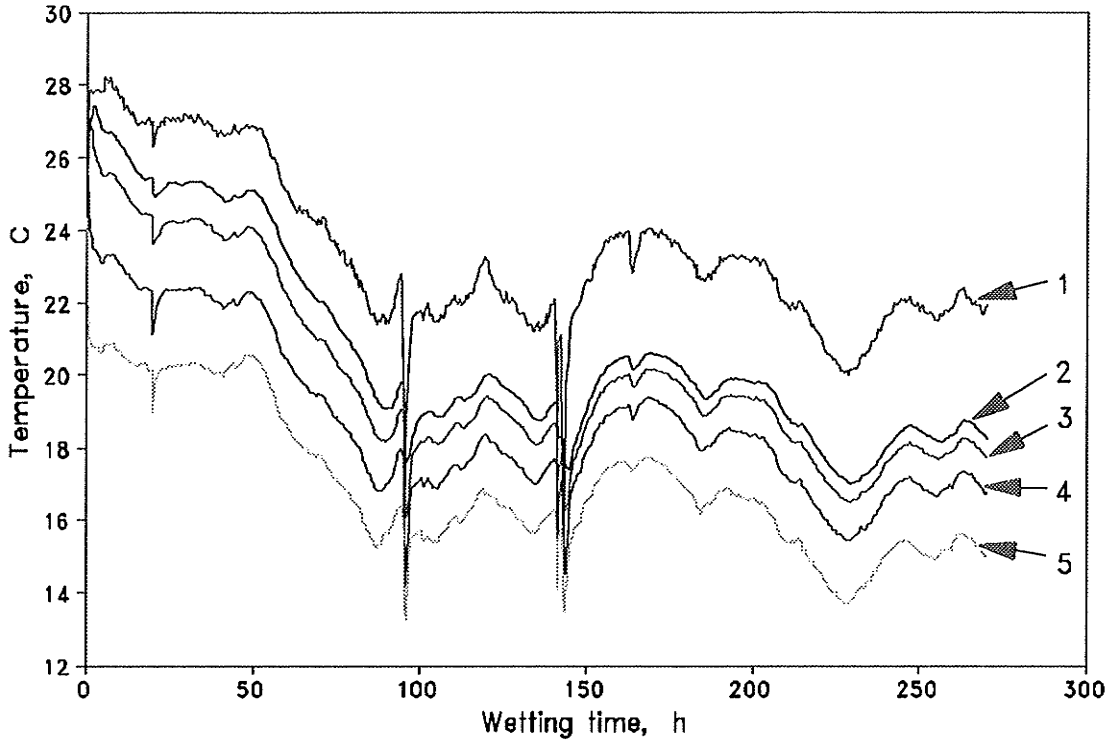

Fig. C1 Temperature change during the first wetting cycle. 1-temperature of ambient air; 2-temperature at top level in the bin; 3-temperature at middle level; 4-temperature at bottom level; 5-temperature of humidified air in plenum.

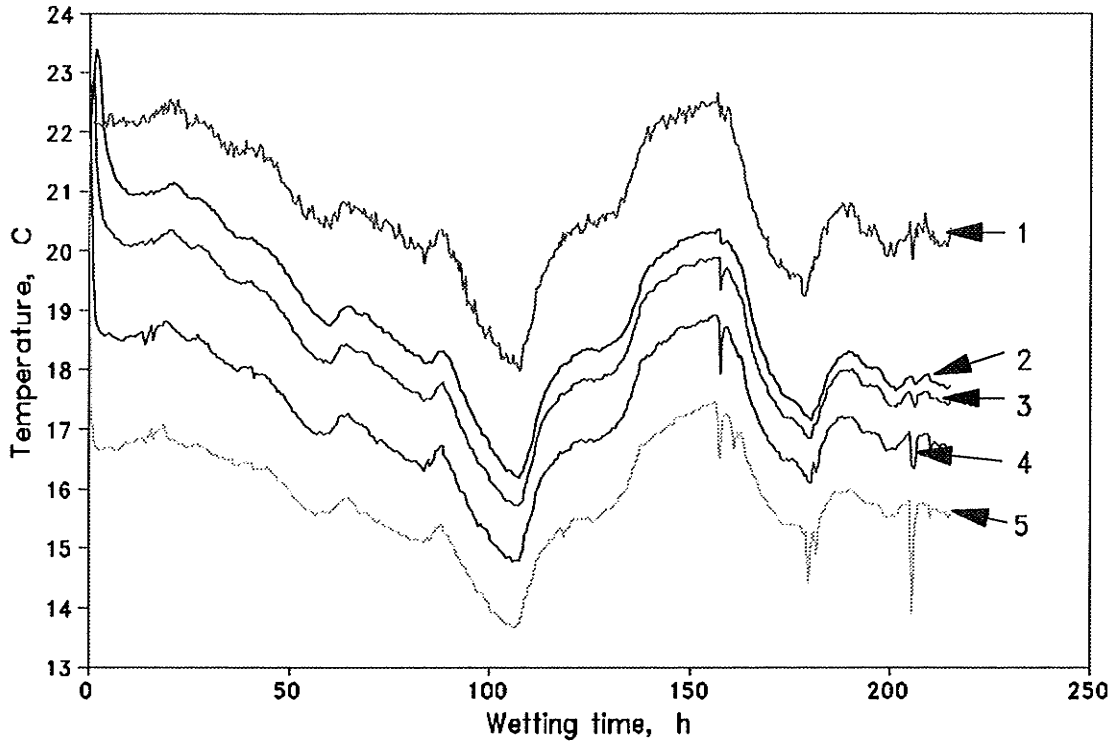

Fig. C2 Temperature change during the third wetting cycle. 1-temperature of ambient air; 2-temperature at top level in the bin; 3-temperature at middle level; 4-temperature at bottom level; 5-temperature of humidified air in plenum.

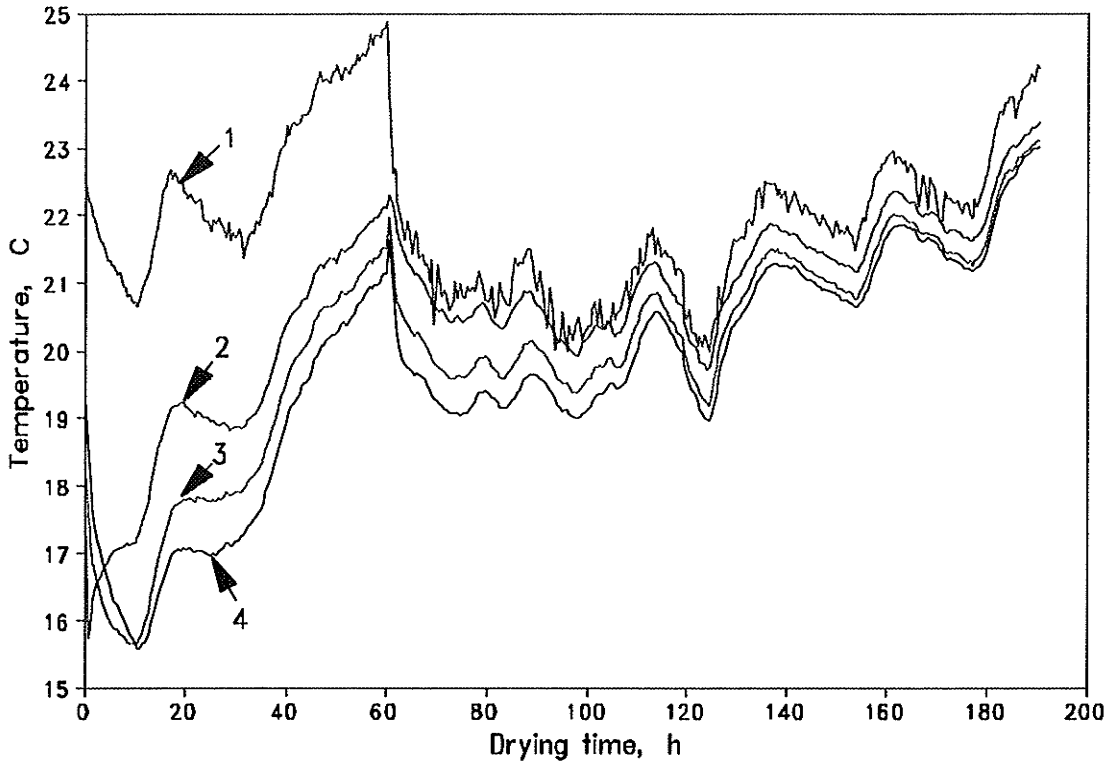

Fig. C3 Temperature change during the second drying cycle. 1-temperature of ambient air; 2-temperature at bottom level; 3-temperature at middle level; 4-temperature at top level.

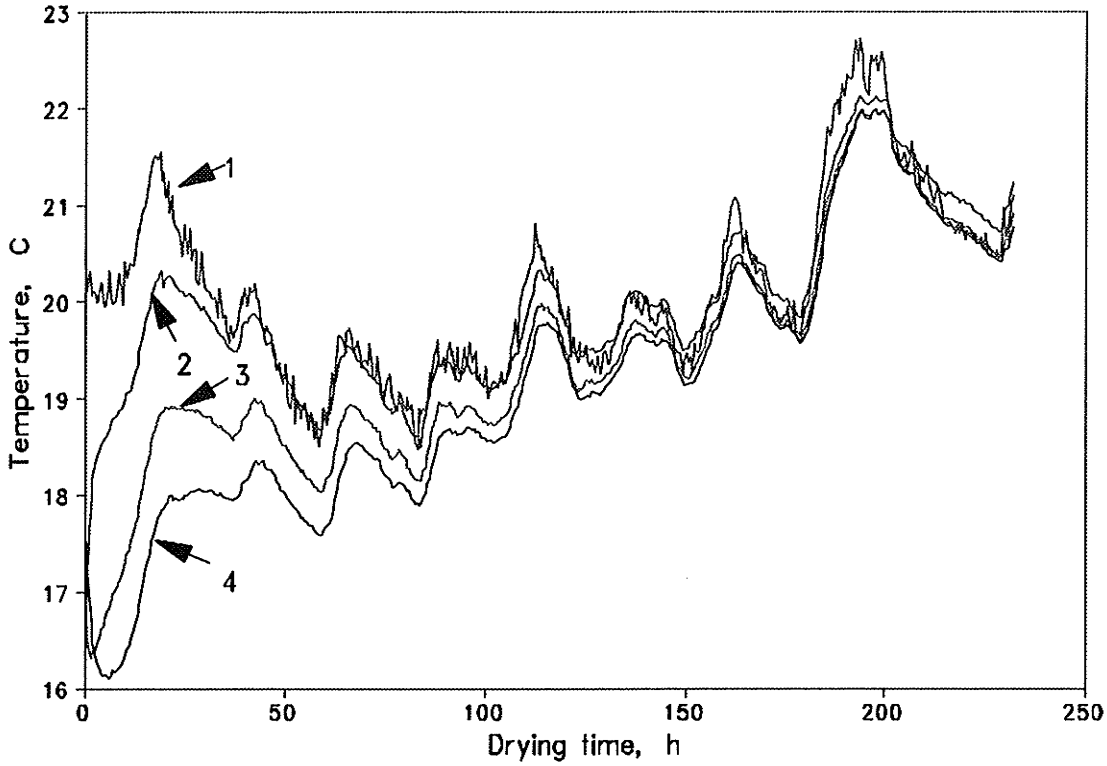

Fig. C4 Temperature change during the fourth drying cycle. 1-temperature of ambient air; 2-temperature at bottom level; 3-temperature at middle level; 4-temperature at top level.

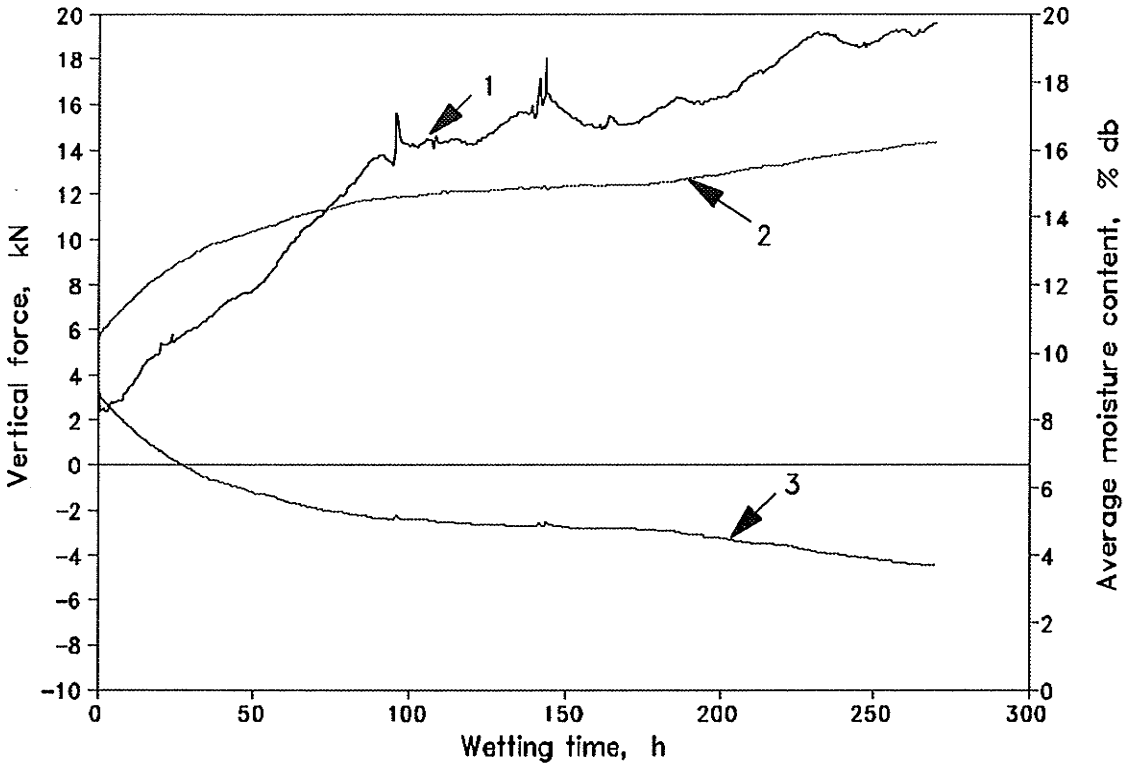

Fig. C5 Vertical forces on the floor and wall during the first wetting cycle. 1-average moisture content of grain; 2-vertical force on floor; 3-vertical force on wall.

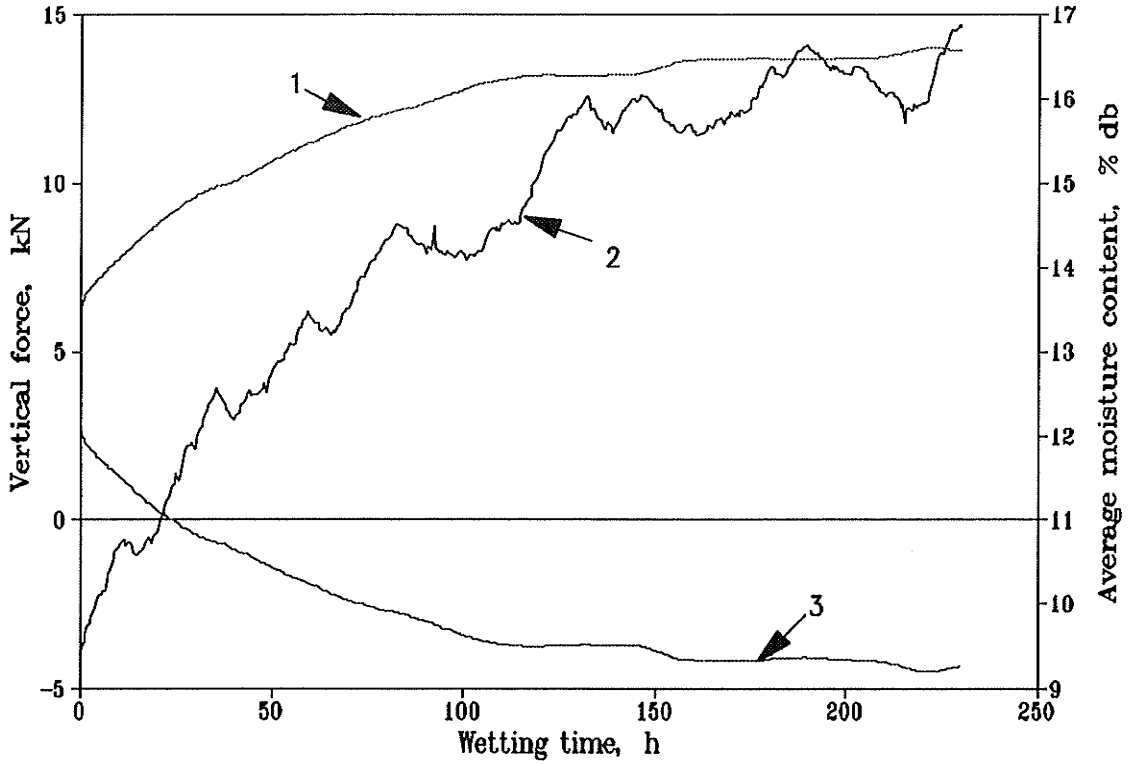

Fig. C6 Vertical forces on the floor and wall during the second wetting cycle. 1-vertical force on floor; 2-average moisture content of grain; 3-vertical force on wall.

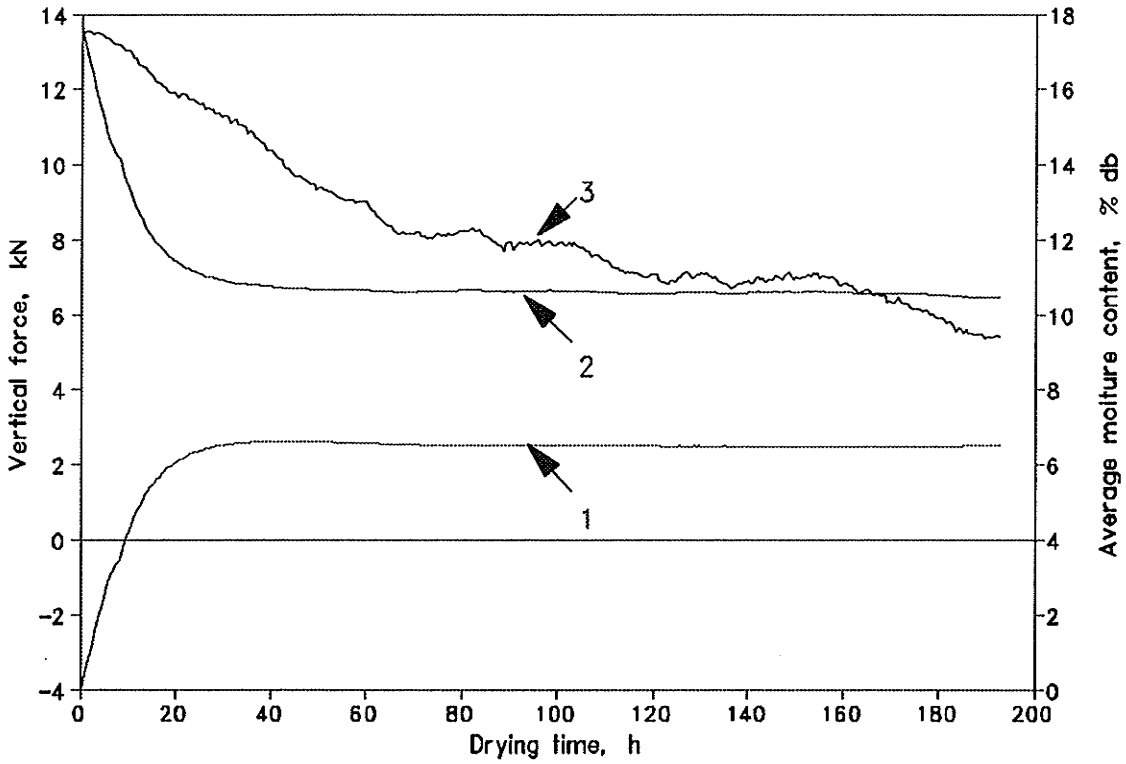

Fig. C7 Vertical forces on the floor and wall during the third drying cycle. 1-vertical force on wall; 2-vertical force on floor; 3-average moisture content of grain.

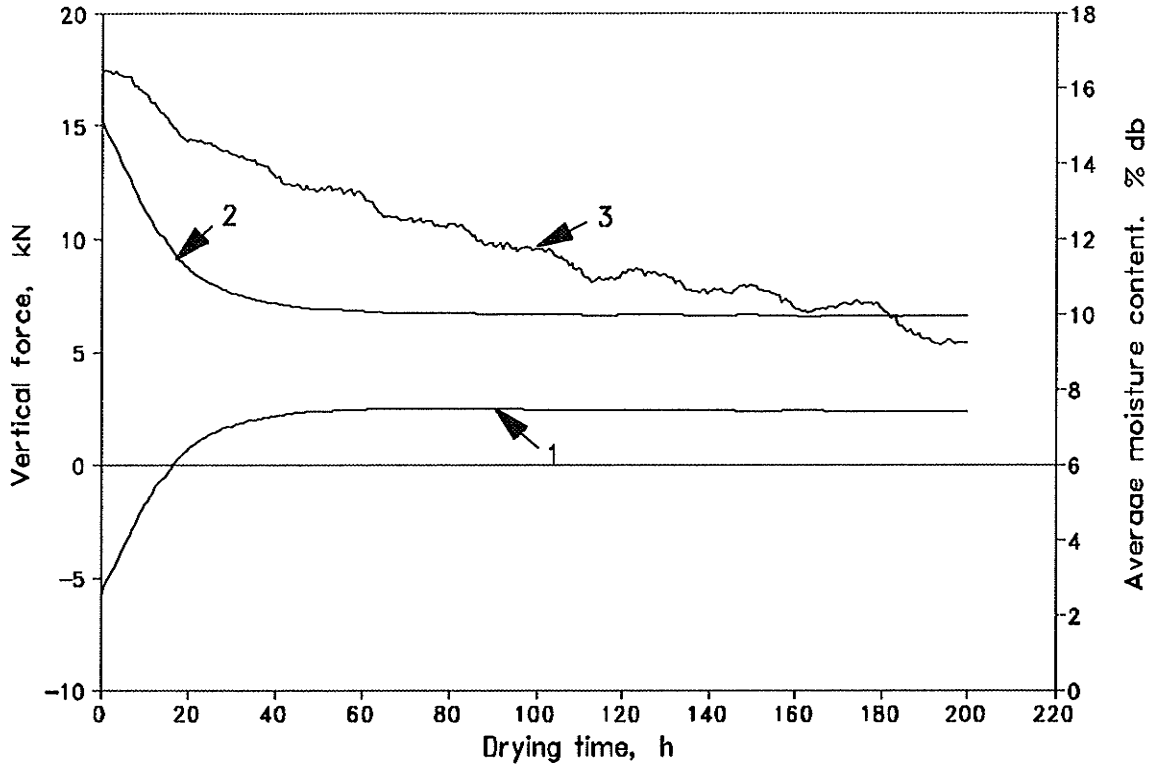

Fig. C8 Vertical forces on the floor and wall during the fourth drying cycle. 1-vertical force on wall; 2-vertical force on floor; 3-average moisture content of grain.

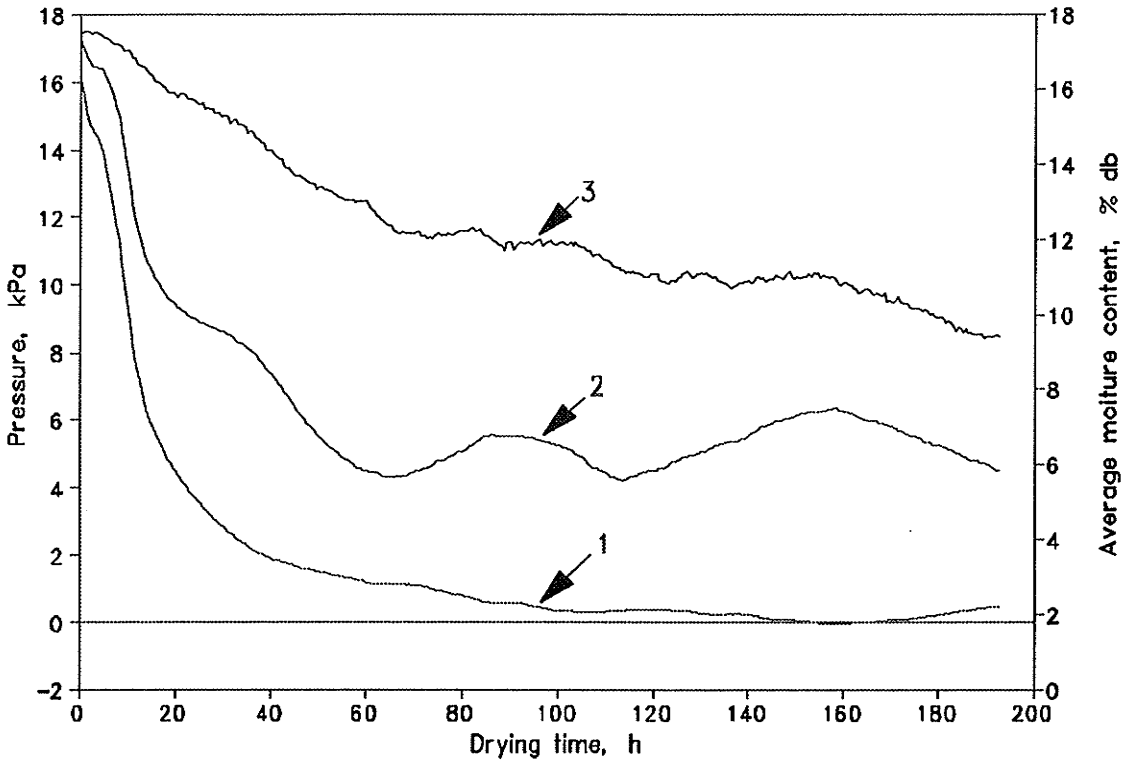

Fig. C9 Lateral and vertical pressures at the top level during the third drying cycle. 1-lateral pressure; 2-vertical pressure; 3-average moisture content of grain.

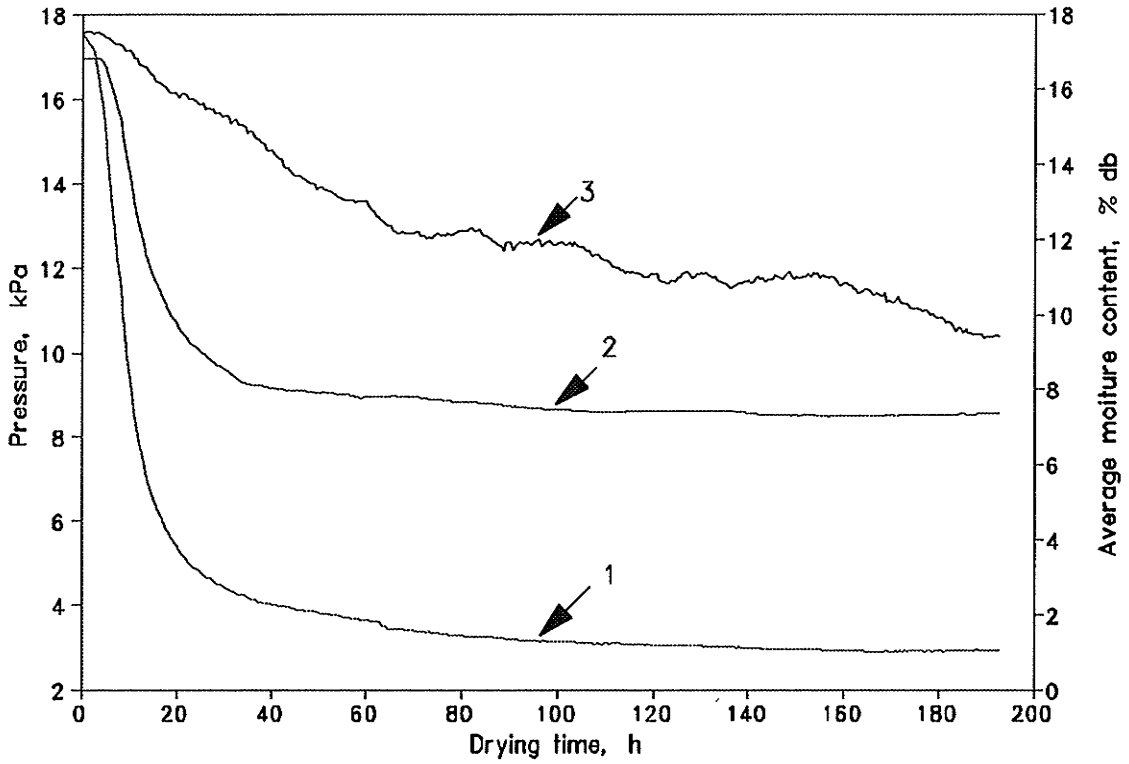

Fig. C10 Lateral and vertical pressures at the middle level during the third drying cycle. 1-lateral pressure; 2-vertical pressure; 3-average moisture content of grain.

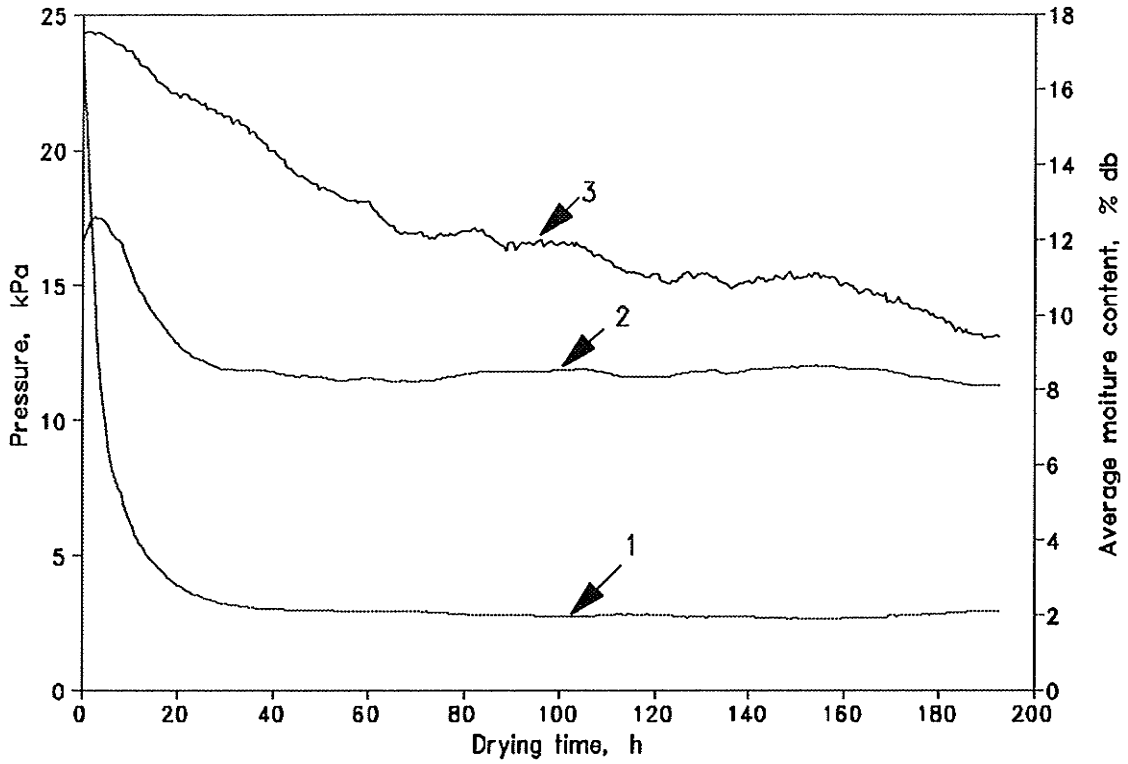

Fig. C11 Lateral and vertical pressures at the bottom level during the third drying cycle. 1-lateral pressure; 2-vertical pressure; 3-average moisture content of grain.

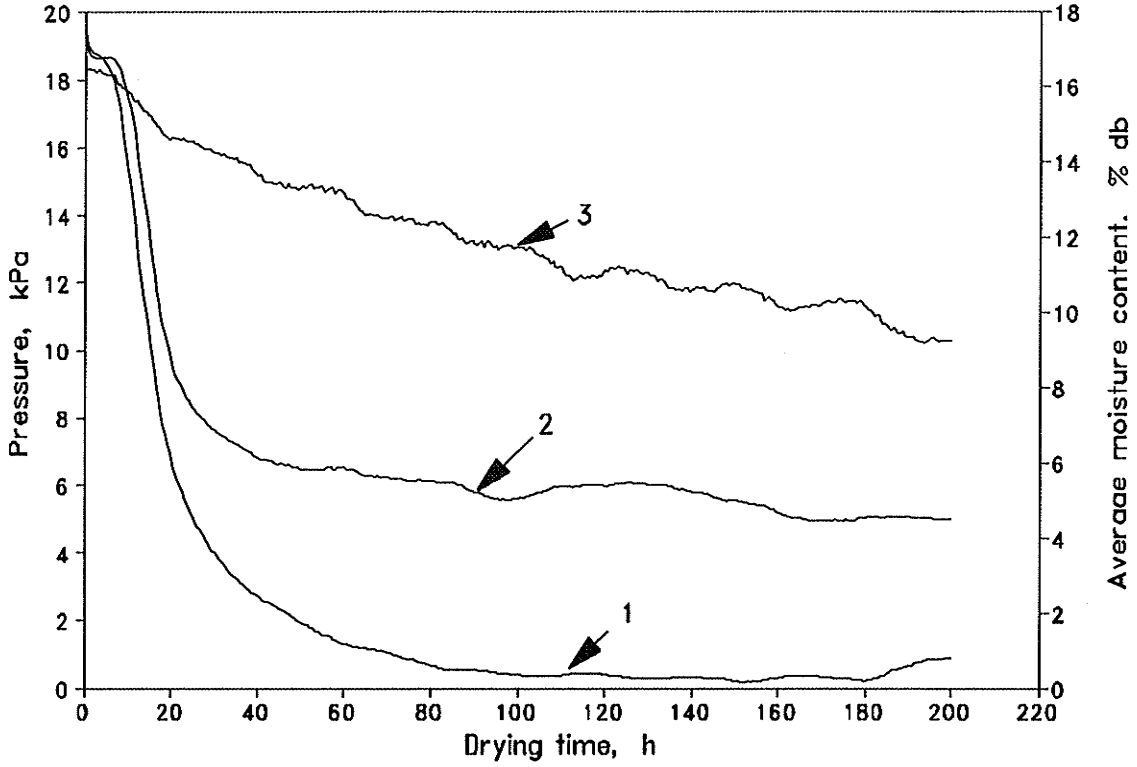

Fig. C12 Lateral and vertical pressures at the top level during the fourth drying cycle. 1-lateral pressure; 2-vertical pressure; 3-average moisture content of grain.

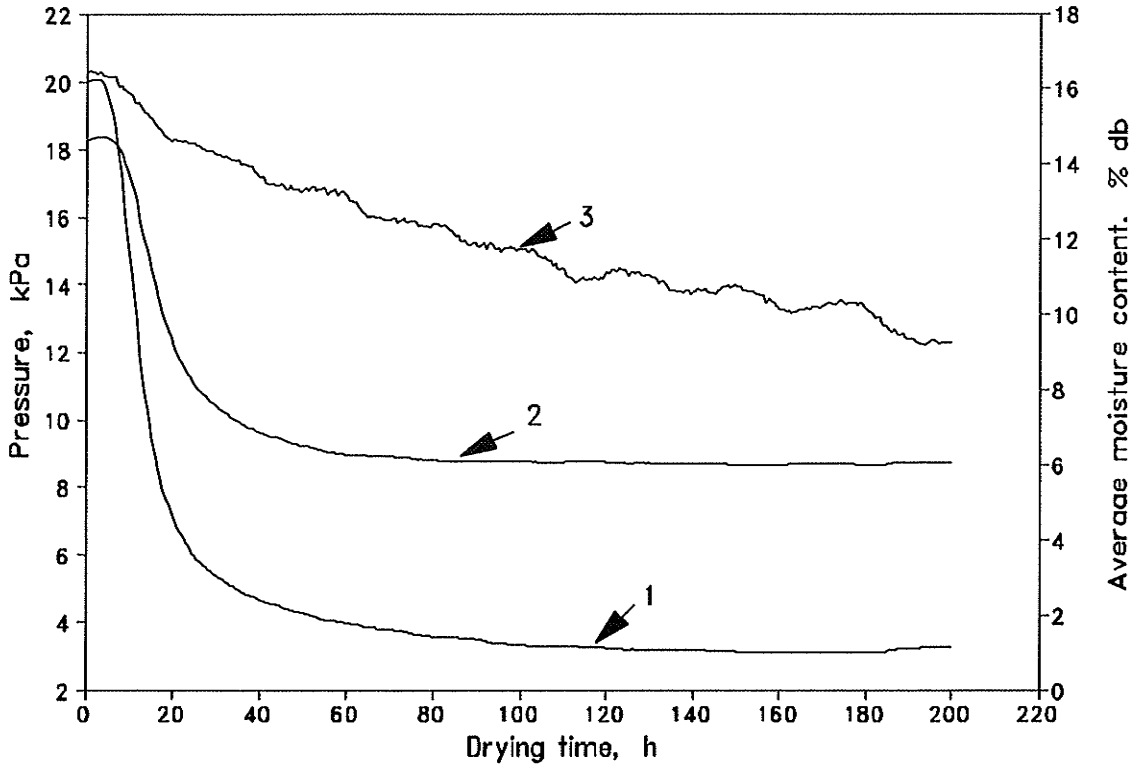

Fig. C13 Lateral and vertical pressures at the middle level during the fourth drying cycle. 1-lateral pressure; 2-vertical pressure; 3-average moisture content of grain.

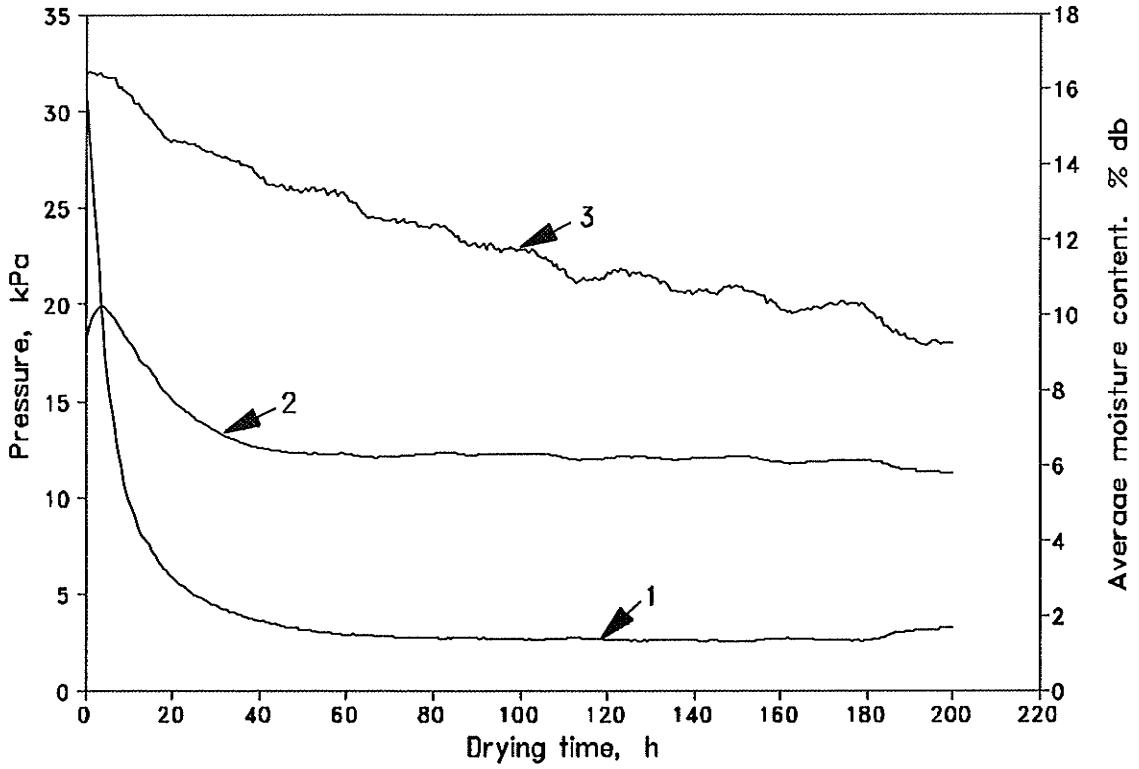

Fig. C14 Lateral and vertical pressures at the bottom level during the fourth drying cycle. 1-lateral pressure; 2-vertical pressure; 3-average moisture content of grain.